Title

In Vitro Biosynthetic Pathway Investigations of Neuroprotectin D1 (NPD1) and Protectin DX (PDX) by Human 12-Lipoxygenase, 15-Lipoxygenase-1, and 15-Lipoxygenase-2

Journal

Biochemistry, 60(22)

ISSN

0006-2960

Authors

Tsai, Wan-Chen
Kalyanaraman, Chakrapani
Yamaguchi, Adriana
et al.

Publication Date

2021-06-08

DOI

10.1021/acs.biochem.0c00931

Peer reviewed

HHS Public Access

Author manuscript

Biochemistry. Author manuscript; available in PMC 2022 April 13.

Published in final edited form as:

Biochemistry. 2021 June 08; 60(22): 1741–1754. doi:10.1021/acs.biochem.0c00931.

In Vitro Biosynthetic Pathway Investigations of Neuroprotectin D1 (NPD1) and Protectin DX (PDX) by Human 12-Lipoxygenase, 15-Lipoxygenase-1, and 15-Lipoxygenase-2

Wan-Chen Tsai,
Department of Chemistry and Biochemistry, University of California, Santa Cruz, Santa Cruz, California 95064, United States

Chakrapani Kalyanaraman,
Department of Pharmaceutical Chemistry, School of Pharmacy, University of California, San Francisco, San Francisco, California 94158, United States

Adriana Yamaguchi,
Department of Pharmacology, University of Michigan Medical School, Ann Arbor, Michigan 48109, United States

Michael Holinstat,
Department of Pharmacology, University of Michigan Medical School, Ann Arbor, Michigan 48109, United States

Matthew P. Jacobson,
Department of Pharmaceutical Chemistry, School of Pharmacy, University of California, San Francisco, San Francisco, California 94158, United States

Theodore R. Holman
Department of Chemistry and Biochemistry, University of California, Santa Cruz, Santa Cruz, California 95064, United States

Abstract

In this paper, human platelet 12-lipoxygenase [h12-LOX (ALOX12)], human reticulocyte 15-lipoxygenase-1 [h15-LOX-1 (ALOX15)], and human epithelial 15-lipoxygenase-2 [h15-LOX-2 (ALOX15B)] were observed to react with docosahexaenoic acid (DHA) and produce 17*S*-hydroperoxy-4*Z*,7*Z*,10*Z*,13*Z*,15*E*,19*Z*-docosahexaenoic acid (17S-HpDHA). The k_{cat}/K_M values with DHA for h12-LOX, h15-LOX-1, and h15-LOX-2 were 12, 0.35, and 0.43 s^{-1} μM^{-1},

Corresponding Author: Theodore R. Holman – Department of Chemistry and Biochemistry, University of California, Santa Cruz, Santa Cruz, California 95064, United States; Phone: +1 831 459 5884; holman@ucsc.edu; Fax: +1 831 459 2935.

Supporting Information

The Supporting Information is available free of charge at https://pubs.acs.org/doi/10.1021/acs.biochem.0c00931.
MS characterization of oxylipin standards and pH dependence of PDX formation (PDF)

Accession Codes

h12-LOX, P18054; h15-LOX-2, O15296; h15-LOX-1, P16050.

Complete contact information is available at: https://pubs.acs.org/10.1021/acs.biochem.0c00931

The authors declare the following competing financial interest(s): M.P.J. is a consultant to and shareholder of Schrodinger LLC, which licenses the software used in this work.

respectively, which demonstrate h12-LOX as the most efficient of the three. These values are comparable to their counterpart k_{cat}/K_M values with arachidonic acid (AA), 14, 0.98, and 0.24 s^{-1} μM^{-1}, respectively. Comparison of their product profiles with DHA demonstrates that the three LOX isozymes produce 11S-HpDHA, 14S-HpDHA, and 17S-HpDHA, to varying degrees, with 17S-HpDHA being the majority product only for the 15-LOX isozymes. The effective k_{cat}/K_M values (k_{cat}/K_M × percent product formation) for 17S-HpDHA of the three isozymes indicate that the *in vitro* value of h12-LOX was 2.8-fold greater than that of h15-LOX-1 and 1.3-fold greater than that of h15-LOX-2. 17S-HpDHA was an effective substrate for h12-LOX and h15-LOX-1, with four products being observed under reducing conditions: protectin DX (PDX), 16*S*,17*S*-epoxy-4*Z*,7*Z*,10*Z*,12*E*,14*E*,19*Z*-docosahexaenoic acid (16S,17S-epoxyDHA), the key intermediate in neuroprotection D1 biosynthesis [NPD1, also known as protectin D1 (PD1)], 11,17S-diHDHA, and 16,17S-diHDHA. However, h15-LOX-2 did not react with 17-HpDHA. With respect to their effective k_{cat}/K_M values, h12-LOX was markedly less effective than h15-LOX-1 in reacting with 17S-HpDHA, with a 55-fold lower effective k_{cat}/K_M in producing 16S,17S-epoxyDHA and a 27-fold lower effective k_{cat}/K_M in generating PDX. This is the first direct demonstration of h15-LOX-1 catalyzing this reaction and reveals an *in vitro* pathway for PDX and NPD1 intermediate biosynthesis. In addition, epoxide formation from 17S-HpDHA and h15-LOX-1 was negatively affected via allosteric regulation by 17S-HpDHA (K_d = 5.9 μM), 12*S*-hydroxy-5*Z*,8*Z*,10*E*,14*Z*-eicosatetraenoic acid (12S-HETE) (K_d = 2.5 μM), and 17*S*-hydroxy-13*Z*,15*E*,19*Z*-docosatrienoic acid (17S-HDTA) (K_d = 1.4 μM), suggesting a possible regulatory pathway in reducing epoxide formation. Finally, 17S-HpDHA and PDX inhibited platelet aggregation, with EC_{50} values of approximately 1 and 3 μM, respectively. The *in vitro* results presented here may help advise *in vivo* PDX and NPD1 intermediate (i.e., 16S,17S-epoxyDHA) biosynthetic investigations and support the benefits of DHA rich diets.

Graphical Abstract

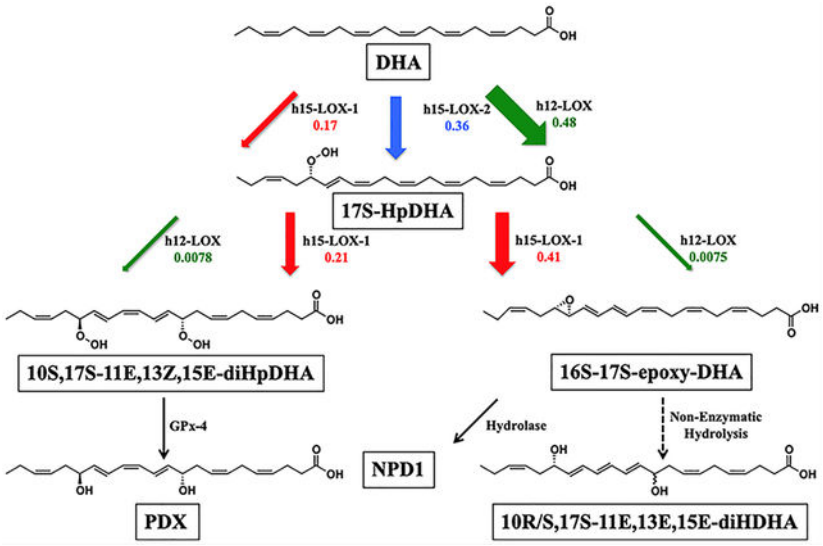

There are two types of inflammation: acute and chronic. Acute inflammation is the initial response of the body to injury and infection and is initiated by neutrophils, eosinophils, and M1-polarized macrophages, which are amplified by bioactive molecules,

such as prostaglandins and leukotrienes.[1] However, an uncontrolled immune response promotes chronic inflammation and unresolved tissue damage.[2,3] At the peak of the acute inflammatory response, the immune cells undergo a temporal lipid mediator class switch and start producing specialized pro-resolving mediators (SPMs).[4,5] To date, more than 20 different SPMs have been identified, and they can be subdivided into six main classes: AA-derived lipoxins (LXs), EPA-derived E-series resolvins (RvEs), DHA-derived D-series resolvins (RvDs), neuroprotectins [i.e., NPD1, also known as protectin-1 (PD1)] and their conjugates (PCTRs), maresins (Mar1) and their conjugates (MCTRs), and DPA-derived 13-series resolvins (RvTs).[3] The failure to undergo the transition from inflammation to resolution has been revealed to cause a variety of chronic inflammatory diseases, such as cardiovascular disease, Alzheimer's disease (AD), amyotrophic lateral sclerosis (ALS), and cancer.[6] Nonsteroidal anti-inflammatory drugs (NSAIDs) have so far been the major therapeutics for acute inflammation by inhibiting the cyclooxygenase (COX) activity; however, these drugs have a limited effect on resolving chronic inflammatory diseases. The challenge for treatment of chronic inflammation is simultaneously inhibiting the pro-inflammatory processes while stimulating the pro-resolution processes. This goal is complicated by the fact that production of both pro-inflammatory and pro-resolving molecules is catalyzed from the same enzymes, lipoxygenase (LOX) and cyclooxygenase (COX) isozymes.[5,7] Therefore, characterizing the specific roles that the LOX and COX isozymes play in the production of SPMs to develop the most effective therapeutic treatment for chronic inflammatory diseases is critical.

Neuroprotectin D1 (NPD1) was the first identified neuroprotective mediator of docosahexaenoic acid (DHA) belonging to the SPMs and was fully assigned by matching the biological sample with stereochemically pure and enantio-enriched isomers obtained by total synthesis.[8] The name "neuroprotectin D1" was based on its neuroprotective bioactivity in brain ischemia reperfusion (BIR) and oxidatively stressed retina pigment epithelial (RPE) cells, as well as its ability to protect cells from oxidative stress-induced apoptosis.[9,10] It can also upregulate the stimulation of the anti-apoptotic protein, Bcl-2, and decrease the level of pro-apoptotic protein, Bax, in ARPE-19 cells during oxidative stress.[9]

Protectin DX (PDX), another SPM and stereoisomer of NPD1, was first obtained enzymatically by Serhan et al. *in vitro*, and then its structure was re-examined later by Butovich et al. to confirm the geometry of the double bonds of the conjugated triene unit and the stereoconfiguration at carbon 10.[11–13] The bioactivity of PDX revealed that it can inhibit inflammation associated with cyclooxygenase (COX) activities, reactive oxygen species (ROS) formation, and influenza virus replication.[14] The biosyntheses of NPD1 and PDX are both proposed to be catalyzed by LOX isozymes; however, the specific LOX isozymes involved and the detailed biosynthetic pathway are not well characterized.

Lipoxygenases (LOX) are non-heme iron-containing enzymes with the primary reactivity of abstracting a hydrogen atom from a *cis*,*cis*-1,4-pentadiene of a polyunsaturated fatty acid (PUFA), followed by oxygen insertion to generate a hydroperoxide product. In humans, there are six LOX isozymes and the naming of specific LOX isozymes is dependent on the carbon of the substrate that becomes oxidized.[15] The oxygenation site depends on which end of the substrate enters the active site first. For example,

human reticulocyte 15-lipoxygenase-1 [h15-LOX-1 (ALOX15)] mostly produces the ω-6 product, 15*S*-hydroperoxy-5*Z*,8*Z*,11*Z*,13*E*-eicosatetraenoic acid (15S-HpETE), from arachidonic acid (AA) and 17*S*-hydroperoxy-4*Z*,7*Z*,10*Z*,13*Z*,15*E*,19*Z*-docosahexaenoic acid (17S-HpDHA) from DHA because the fatty acid substrate enters the active site methyl end first (Figure 1).

LOX isozymes also perform dehydration reactions when the hydroperoxide oxylipin is the substrate, to produce an epoxide intermediate. The hydrogen atom on the bis-allylic methylene carbon is abstracted, generating a septa-dienyl radical, but instead of oxygen attacking the septa-dienyl radical intermediate, the epoxide is formed by hydroperoxide dehydration. This dehydration mechanism is observed in the reaction of human reticulocyte 15-LOX-1 [h15-LOX-1 (ALOX15)] or human platelet 12-LOX [h12-LOX (ALOX12)] with 5S,15S-diHpETE to form the 14,15-epoxide intermediate, which is then converted to lipoxin B4 (LXB_4).[16]

Both LOX oxygenation and dehydration reactions are proposed for the biosynthesis of NPD1. h15-LOX-1 first generates 17S-HpDHA, and then a hydrogen atom is abstracted from the ω-11 carbon, which is dehydrated to form the critical NPD1 intermediate, 16*S*,17*S*-epoxy-4*Z*,7*Z*,10*Z*,12*E*,14*E*,19*Z*-docosahexaenoic acid (16S,17S-epoxyDHA). This epoxide is then hydrolyzed enzymatically to form the final product, NPD1 (Figure 1).[17] In addition to h15-LOX-1, both h12-LOX and human epithelial 15-LOX-2 [h15-LOX-2 (ALOX15B)] could also be considered as biocatalysts for NPD1 production due to their known DHA reactivity. While h12-LOX mostly generates the ω-9 product, 14S-HpDHA, it also produces the ω-6 side product, 17S-HpDHA.[18] h15-LOX-2 exhibits reaction specificity similar to that of h15-LOX-1 with the ω-6 oxygenation product, 17S-HpDHA, as the dominant product. Nevertheless, the dehydration step to generate the 16S,17S-epoxyDHA has not been reported for either h12-LOX or h15-LOX-2.[19] With regard to PDX, soybean LOX has been shown to produce it by double oxygenation of DHA, with subsequent reduction to the dialcohol.[12] The ability of h12-LOX, h15-LOX-1, and h15-LOX-2 to generate 17S-HpDHA indicates that they could participate in the biosynthesis of PDX; however, the subsequent production of 10S,17S-diHpDHA is less obvious because human LOXs manifest unusual LOX reactivity with oxylipins.[20,21]

To investigate possible biosynthetic pathways for both NPD1 and PDX, the reactivities and kinetics of h12-LOX, h15-LOX-1, and h15-LOX-2 were investigated with the goal of determining their relative *in vitro* biosynthetic properties. Understanding which LOX isoenzyme is involved in the *in vitro* biosynthesis of NPD1 and PDX may help with the interpretation of their *in vivo* biosynthetic pathways and thus help understand the cellular consequences of specific LOX inhibition in the treatment of human diseases.

MATERIALS AND METHODS

Chemicals.

4*Z*,7*Z*,10*Z*,13*Z*,16*Z*,19*Z*-Docosahexaenoic acid (DHA) and 13*Z*,16*Z*,19*Z*-docosatrienoic acid (DTA) were purchased from Nu Chek Prep, Inc., at >99% purity. Oxylipin mass spectrometry standards were purchased from Cayman Chemicals. All other solvents and

chemicals were of reagent grade or better and purchased from Fisher Scientific (Pittsburgh, PA) and used as purchased without further purification.

Synthesis and Purification of Oxylipins.

17*S*-Hydro-peroxy-4*Z*,7*Z*,10*Z*,13*Z*,15*E*,9*Z*-docosahexaenoic acid (17S-HpDHA) was made from the reaction of DHA (50 μM) with soybean lipoxygenase-1 (sLOX-1) in 200 mL of 50 mM borate buffer (pH 9.2). The absorbance was monitored at 234 nm until the reaction was completed and quenched with 1% (v/v) glacial acetic acid. The reaction mixture was extracted three times with 200 mL of dichloromethane (DCM) and then concentrated under reduced pressure. The crude product was resuspended with 250 μL of methanol and purified isocratically via high-performance liquid chromatography (HPLC) on a Higgins Haisil Semipreparative (5 μm, 250 mm × 10 mm) C18 column with a 60:40 mixture of 99.9% acetonitrile with 0.1% acetic acid and 99.9% water with 0.1% acetic acid, with a flow rate of 2 mL/min. 17*S*-Hydroxy-4*Z*,7*Z*,10*Z*,13*Z*,15*E*,9*Z*-docosahexaenoic acid (17S-HDHA) was synthesized as previously described for 17S-HpDHA, but with the reductant, trimethyl phosphite, added prior to HPLC. 12*S*-Hydroxy-5*E*,8*Z*,10*Z*,14*Z*-eicosatetraenoic acid (12S-HETE) was synthesized from the reaction of AA (50 μM) with h12-LOX in 200 mL of 25 mM HEPES buffer (pH 8.0). The purity of the isolated products was assessed via LC-MS/MS to be >90%, with the following parameters: 17S-HpDHA (UV_{max} = 237 nm, parent *m*/*z* 359.2, major MS/MS fragments *m*/*z* 341 and 245), 17S-HDHA (UV_{max} = 237 nm, parent *m*/*z* 343.2, major MS/MS fragments *m*/*z* 281 and 245), and 12S-HETE (UV_{max} = 234 nm, parent *m*/*z* 319.2, major MS/MS fragments *m*/*z* 301 and 179).

h12-LOX and h15-LOX-1 Expression and Purification.

The overexpression and purification of h15-LOX-1,[22] h12-LOX,[22] and h15-LOX-2[23] were performed as previously described. Briefly, h15-LOX-1, h12-LOX, and h15-LOX-2 were expressed as fusion proteins with a six-His TAG on the N-terminus and purified by FPLC (Bio-Rad) with an affinity nickel-iminodiacetic acid agarose column (4 °C). The purities of h15-LOX-1, h12-LOX, and h15-LOX-2 were determined by sodium dodecyl sulfate–polyacrylamide gel electrophoresis analysis to be >90%. The iron content of all of the enzymes was assessed on the Thermo Element XR inductively coupled plasma mass spectrometry (ICP-MS) instrument via comparison with an iron standard solution. Cobalt-EDTA was used as an internal standard.

Steady-State Kinetics of h12-LOX, h15-LOX-1, or h15-LOX-2 with DHA, 17S-HpDHA, and 17S-HDHA.

h15-LOX-1 reactions were performed in a 1 cm quartz cuvette containing 2 mL of 25 mM HEPES buffer (pH 7.5) with a substrate (DHA, 17S-HpDHA, or 17S-HDHA), and mixtures stirred constantly. h12-LOX and h15-LOX-2 reactions were performed in a manner similar to that of the h15-LOX-1 reactions, but the reaction pH was 8.0. The reactions were initiated by adding approximately 40 nM enzyme to a 2 mL reaction mixture containing 1–20 μM DHA, 1–50 μM 17S-HpDHA, or 1–100 μM 17S-HDHA. For the DHA reactions, the formation of the conjugated diene products was monitored at 237 nm (ε = 25000 M^{-1} cm^{-1}) with the PerkinElmer Lambda 40 UV/vis spectrophotometer. The 17S-HpDHA and 17S-HDHA reactions were monitored simultaneously on the Hewlett-

Packard 8453 diode-array spectrophotometer at 270 nm for 10S,17S-diHpDHA, 10*R*/*S*,17*S*-dihydroxy-4*Z*,7*Z*,11*E*,13*E*,15*E*,19*Z*-docosahexaenoic acid (10R/S,17S-EEE-diHDHA), and 16,17S-diHpDHA formation using the estimated extinction coefficient for a conjugated triene in buffer (ε_{270} = 40000 M^{-1} cm^{-1}).[24] It should be noted that 11,17S-diHpDHA has two unconjugated diene moieties, which we observe to have a λ_{max} of 238 nm (Figure S1). The chromophore for 11,17S-diHpDHA is similar to that of the previously published methyl ester 9,15-diHpETE,[25] and we used the published extinction coefficient in methanol (ε_{238} =49600 M^{-1} cm^{-1}).[25] It should be noted that the mono-hydroperoxides are produced from the alcohol substrate, but the dihydroperoxides are produced from the hydroperoxide substrate, with the same ε values used for both. Kinetic parameters were calculated by using KaleidaGraph to fit initial rates, at <20% turnover.

Product Analysis of LOX Isozyme Reactions with DHA, 17S-HpDHA, and 17S-HDHA.

DHA (10 μM), 17S-HpDHA (1 μM), or 17S-HDHA (1 μM) was reacted with 300 nM h12-LOX, h15-LOX-1, or h15-LOX-2 in 2 mL of 25 mM HEPES buffer (pH 7.5 for h15-LOX-1 and pH 8.0 for h12-LOX and h15-LOX-2) for 3–10 min as monitored by an ultraviolet–visible (UV–vis) spectrophotometer. The reactions were quenched with 1% (v/v) glacial acetic acid, and mixtures extracted three times with 2 mL of dichloromethane (DCM). The reactions were performed in parallel with the enzyme absent as a control for background oxidation. In addition to the native reaction mixtures, a reaction mixture was reduced with trimethyl phosphite for comparison. The products were dried under a stream of N_2 gas, reconstituted in 100 μL of a 50:50 acetonitrile/water mixture with 0.1% formic acid, and injected into an LC-MS/MS system consisting of a Sciex x500B qTOF instrument, equipped with a Sciex ExcionLC HPLC system, using a C_{18} column (Phenomenex Kinetex, 4 μm, 150 mm × 2.0 mm). Mobile phase A consisted of water with 0.1% (v/v) formic acid, and mobile phase B was acetonitrile with 0.1% (v/v) formic acid. The column was run isocratically with a 60:40 mixture of mobile phase A and mobile phase B, with a flow rate of 0.400 mL/min. Analytes were ionized through electrospray ionization with a −4.0 kV spray voltage and 50, 50, and 20 psi for ion source gases 1 and 2 and curtain gas, respectively. The CAD (collisionally activated dissociation) gas was set to 7, and the probe temperature was 550 °C. MS/MS acquisition was performed using SWATH and *m*/*z* ratios of ±0.5, and the parent masses used for the HDHA and diHDHA products were *m*/*z* 343.2 and 359.2, respectively. All analyses were performed in negative ionization mode at the normal resolution setting. The products were identified by matching their retention times, UV spectra, and MS/MS patterns to those of PDX (270 nm, *m*/*z* 359.2, 341.21, 323.20, 315.23, 297.22, 290.15, 279.21, 272.14, 261.15, 243.14, 227.14, 206.13, 199.15, 188.12, 181.10, 177.13, 159.12, 153.09, 137.06, and 107.09). The molecules without standards were deduced from comparison to theoretical fragments, and their double bond geometry was determined through their UV spectra: 11,17-diHDHA (238 nm, *m*/*z* 359.22, 341.21, 323.20, 315.23, 297.22, 290.15, 279.21, 272.14, 261.15, 243.14, 227.14, 199.15, 194.09, 193.09, 165.13, 149.10, 147.12, 121.10, and 95.05), 10,17-diHDHA (270 nm, *m*/*z* 359.2, 341.21, 323.20, 315.23, 297.22, 290.15, 279.21, 272.14, 261.15, 243.14, 227.14, 206.13, 199.15, 188.12, 181.10, 177.13, 159.12, 153.09, 137.06, and 107.09), and 16,17-diHDHA (234 nm, *m*/*z* 359.2, 297.22, 279.21, 272.14, 261.15, 243.14, 231.14, 217.16, 199.15, and 187.12). In the case of 11,17-diHDHA, it was compared to 11,17-diHDHA generated by reacting

soybean LOX-1 with 11*R*/*S*-HDHA (Cayman Chemicals) and their retention times, UV spectra, and MS spectra were identical (*vide infra*).

It should be noted that the products were not absolutely quantitated via LC-MS/MS, and hence, internal standards and calibration curves were not utilized. Rather, their relative ratios were determined by area analysis of the parent mass, assuming each of the doubly oxygenated oxylipins had the same detector response. These relative areas were confirmed with MRM traces: 11,17S-diHDHA (*m*/*z* 359.2 → 147.1), 10R/S,17S-EEE-diHDHA (*m*/*z* 359.2 → 153.1), PDX (*m*/*z* 359.2 → 153.1), and 16,17S-diHDHA (*m*/*z* 359.2 → 231.1).

Allosteric Regulation of Epoxidation of h15-LOX-1 and h12-LOX.

The allosteric effects were investigated using varied concentrations of 17S-HpDHA (1–50 μM) and h15-LOX-1 (0.2 μM) with a 10 min reaction. In addition, 12S-HETE or 17*S*-hydroxy-13*Z*,15*E*,19*Z*-docosatrienoic acid (17S-HDTA) was added at varying concentrations (1–25 μM), with 1 μM 17S-HpDHA and the product percentages were calculated ($N = 3$). Products were reduced and analyzed via LC-MS as described previously in the product analysis section.

Effect of 17S-HpDHA on Human Platelet Aggregation and Lipidomics.

The University of Michigan Institutional Review Board approved all research involving human volunteers. A written informed consent was obtained from self-reported healthy donors prior to the blood draws. Whole blood was collected via venipuncture into vacutainers containing sodium citrate (3.2%; Greiner Bio-One, Monroe, NC). Platelets were isolated through serial centrifugation. Platelet rich plasma was treated with acid citrate dextrose (2.5% sodium citrate basic, 1.5% citric acid, and 2.0% D-glucose) and apyrase (0.02 unit/mL) and then centrifuged for 10 min at 2000*g* to pellet the platelets.[26] Tyrode's buffer (10 mM *N*-2-hydroxyethylpiperazine-N9-2-ethanesulfonic acid, 12 mM sodium bicarbonate, 127 mM sodium chloride, 5 mM potassium chloride, 0.5 mM monosodium phosphate, 1 mM magnesium chloride, and 5 mM glucose) was used at a density of 3×10^8 platelets/mL as determined by a complete blood cell counter (Hemavet 950FS; Drew Scientific, Miami Lakes, FL). For aggregation assays, 250 μL of washed human platelets (3×10^8 platelets/mL) was incubated with 1–10 μM 17S-HpDHA, 10R/S,17S-EEE-diHDHA, PDX, or the control oxylipin, 12*S*-hydroxy-8*Z*,10*E*,14*Z*-eicosatrienoic acid (12S-HETrE), for 10 min at 37 °C in a glass cuvette. The oxylipin-treated platelets were stimulated with 0.25 μg/mL collagen while being stirred at 1100 rpm in a Chrono-log model 700 aggregometer, and aggregation was analyzed via a decrease in light transmittance. For lipidomics, 1×10^9 platelets were resuspended in 1 mL of Tyrode's buffer, incubated with 3 μM 17S-HpDHA for 10 min, and stimulated with collagen. Supernatants and pellets from washed platelets were acidified with HCl and extracted three times with 2 mL of DCM and 50 ng of d_5-MaR1 as an internal standard. The reaction mixtures were treated with trimethyl phosphite as the reductant, blown down under a stream of N_2, and resuspended in 500 μL of H_2O with 0.1% formic acid and acetonitrile at a 1:4 ratio. The proteins were precipitated out by freezing the samples in a −80 °C freezer for 20 min and then spinning them down at 13K for 15 min. The supernatants were removed and dried under N_2. The samples were reconstituted in acetonitrile and H_2O with 0.1% formic acid (50:50 ratio) and analyzed by

LC-MS/MS, as described above. The *m*/*z* transitions used for 10,17-diHDHA isomers were *m*/*z* 359.2 → 153.1, as described above.

Molecular Docking.

The homology model of h15-LOX-1 was constructed with the substrate-mimetic inhibitor-bound porcine 12-LOX structure (Protein Data Bank entry 3rde) by using PRIME homology modeling software (Schrodinger Inc.).[18] The metal ion (Fe^{3+}), the iron-coordinated hydroxide ion, and the co-crystallized inhibitor were retained during homology modeling. Prior to docking, the model was subjected to a protein preparation step using Protein Preparation Wizard (Schrodinger Inc.). The hydrogen atoms were optimized to make better hydrogen bonding interactions. Protonation states of titratable residues were assigned. Rotameric states of Asn, Gln, Ser, Thr, and Tyr residues were optimized. The model was energy-minimized with restraints, such that heavy atoms did not move beyond 0.3 Å. The three-dimensional (3D) structure of 17S-HpDHA was prepared from the SMILES string using LigPrep software (Schrodinger Inc.). Both the neutral and charged carboxylic acid forms of the substrate were generated, but neither protonation state of the substrate successfully docked to the active site using the standard rigid receptor docking using Glide (Schrodinger Inc.). Therefore, we used InducedFit docking to predict conformational changes necessary to accommodate these ligands. The metal ion, hydroxide ion, and metal ion-coordinating residues (His360, His365, His540, His544, and Ile662) were kept fixed during the InducedFit docking; all other active site residue side chains, as well as the substrate, were sampled extensively. During InducedFit docking, the extra-precision (XP) scoring function was used for Glide redocking. The InducedFit score was used for ranking docking poses.

RESULTS

Production of 17S-HpDHA, Neuroprotectin D1 (NPD1), and the PDX Intermediate, through h15-LOX-1, h15-LOX-2, and h12-LOX.

The biosynthesis of the potent anti-inflammatory molecules, NPD1 and PDX, is dependent on the production of the intermediate, 17*S*-hydroperoxy-4*Z*,7*Z*,10*Z*,13*Z*,15*E*,19*Z*-docosahexaenoic acid (17S-HpDHA). To generate 17S-HpDHA from DHA by LOX isozymes, the hydrogen atom on C15 (*ω*-8) must be abstracted, with a subsequent oxygen insertion at C17 (*ω*-6). h12-LOX, h15-LOX-1, and h15-LOX-2 could produce 17S-HpDHA from DHA, as determined by LC-MS/MS, and therefore, their product profiles and steady-state kinetics were determined to establish the specificity and catalytic efficiency of these reactions.

Product Profile and Steady-State Kinetics of h15-LOX-1 with DHA.

The product profile for the reaction of DHA with h15-LOX-1 showed 17S-HpDHA (49 ± 2%), 14S-HpDHA (37 ± 2%), and 11S-HpDHA (14 ± 2%) (Table 1), consistent with previous work with the purified enzyme.[18,19] These results are also in agreement with the studies that found h15-LOX-1 is capable of making both the *ω*-6 and *ω*-9 oxylipins when using AA as the substrate, 15S-HpETE and 12S-HpHETE, respectively. However, the increased level of production of the *ω*-9 oxylipin with DHA as the substrate (37%

14S-HpDHA vs 10% 12S-HpETE) supports the hypothesis that the increased level of unsaturation and aliphatic chain length of DHA allow for an active site insertion deeper than that of AA, as has been seen previously.[18,21] With regard to the kinetics of h15-LOX-1 and DHA, the k_{cat}/K_M was determined to be 0.35 ± 0.08 μM^{-1} s^{-1}, which was 3-fold slower than that of AA. The k_{cat} was observed to be 2.3 ± 0.6 s^{-1}, only 2-fold less than the rate seen with AA, indicating DHA is a substrate comparable to AA with h15-LOX-1 (Table 2).

Product Profile and Steady-State Kinetics of h15-LOX-2 with DHA.

The product preference for h15-LOX-2 with DHA revealed the production of 17S-HpDHA (84 ± 1%) as the major product and 14S-HpDHA (16 ± 1%) as the minor product (Table 1). This result is consistent with the preference of h15-LOX-2 to abstract a hydrogen atom from the ω-8 carbon with oxygenation on the ω-6 carbon; however, the high percentage of 14S-HpDHA is unusual. In the case of AA, h15-LOX-2 produces only the ω-6 product, 15S-HpETE, which supports the hypothesis that unsaturation and an increased length allow DHA to insert deeper into the h15-LOX-2 active site, as seen with h15-LOX-1 (*vide supra*).[19] For kinetics, the k_{cat}/K_M of this reaction was measured to be 0.43 ± 0.03 μM^{-1} s^{-1}, which is similar to that with AA (k_{cat}/K_M = 0.24 ± 0.02 μM^{-1} s^{-1}). The k_{cat} for DHA was found to be 4.2 ± 0.3 s^{-1}, which is also comparable to that of AA (k_{cat} = 2.5 ± 0.3 s^{-1}) (Table 2).

Product Profile and Steady-State Kinetics of h12-LOX with DHA.

The product distribution of h12-LOX with DHA was also examined by LC-MS/MS and revealed 17S-HpDHA (4 ± 1%), 14S-HpDHA (78 ± 1%), and 11S-HpDHA (18 ± 1%) (Table 1), consistent with previous work,[18] in which the majority product is from abstraction from the ω-11 carbon, with oxygenation on the ω-9 carbon. As seen with both h15-LOX-1 and h15-LOX-2, DHA inserts deeper into the active site, producing an increased percentage of the ω-12 product, 11S-HpDHA. The value of k_{cat}/K_M was determined to be 12 ± 2 μM^{-1} s^{-1}, and the k_{cat} was found to be 14 ± 0.5 s^{-1}, which are both comparable to rates of h12-LOX with AA (k_{cat}/K_M = 14 ± 0.5 μM^{-1} s^{-1}, and k_{cat} = 17 ± 0.5 s^{-1}).[26] From these results, we conclude that DHA is a kinetic substrate for h12-LOX comparable to AA (Table 2).

In summary, AA and DHA are comparable kinetic substrates for the three LOX isozymes, h15-LOX-1, h15-LOX-2, and h12-LOX, as seen by their kinetic values being within 5-fold of each other. However, the product profiles differ dramatically between AA and DHA, indicating that the structural differences between the substrates affect their active site binding configuration.

Effective k_{cat}/K_M for the Production of 17S-HpDHA from DHA and h15-LOX-1, h15-LOX-2, or h12-LOX.

Upon comparison of the effective k_{cat}/K_M (i.e., the k_{cat}/K_M × percent product) of 17S-HpDHA, NPD1, and the PDX precursor, the results revealed that h15-LOX-1, h15-LOX-2, and h12-LOX had comparable catalytic efficiencies. The efficiency of h12-LOX is 2.8-fold greater than that of h15-LOX-1 (Table 3) and 1.3-fold greater than that of h15-LOX-2. Because 17S-HpDHA is the minor h12-LOX product with DHA, it is surprising that a

similar abstraction from the ω-8 carbon, with oxygen insertion at the ω-6 position, is not observed with AA as the substrate (i.e., 12S-HpETE).

Synthesis of the NPD1 Intermediate, 16S,17S-EpoxyDHA, and 10*S*,17*S*-Dihydroxy-4*Z*,7*Z*,11*E*,13*Z*,15*E*,19*Z*-docosahexaenoic acid (PDX) from 17S-HpDHA.

The NPD1 biosynthetic pathway is proposed to be initiated by hydrogen abstraction on C12 of 17S-HpDHA by a lipoxygenase isozyme, whose radical intermediate is dehydrated to form 16S,17S-epoxyDHA, which in turn is enzymatically hydrolyzed to NPD1.[8] In contrast, the biosynthetic pathway for the production of PDX is proposed to proceed through the oxygenation of 17S-HpDHA (or 17-HDHA) on C10 by a LOX isozyme, which is subsequently reduced by GPx-4 to produce PDX.[29] Given the potent biological actions of NPD1 and PDX, we investigated the possible *in vitro* biosynthetic pathways for both molecules to propose possible *in vivo* biosynthetic routes for NPD1 and PDX biosynthesis.

Product Profile and Steady-State Kinetics of h15-LOX-1 and h15-LOX-2 with 17S-HpDHA and 17S-HDHA.

The reaction of h15-LOX-1 with 17S-HpDHA produced a majority of the non-enzymatic hydrolysis products of 16S,17S-epoxyDHA, 10R/S,17S-EEE-diHDHA (54 ± 3%) (Table 4).[17] This non-enzymatic hydrolysis product with EEE conjugation was determined by its reduced nature (di-OH) in a nonreducing environment (Figure S2) and its UV_{max} at ~270 nm, whose shoulder at ~280 nm is slightly higher than the shoulder at ~260 nm, consistent with literature values[30] (Figure S1). Its fragmentation pattern matched the predicted fragments [*m*/*z* 359.2, 341.21, 323.20, 315.23, 297.22, 290.15, 279.21, 272.14, 261.15, 243.14, 227.14, 206.13, 199.15, 188.12, 181.10, 177.13, 159.12, 153.09, 137.06, and 107.09 (Figure S3)]. Under reducing conditions, three oxygenation products were also observed, PDX (28 ± 3%), 11,17*S*-dihydroxy-4*Z*,7*Z*,9*E*,13*Z*,15*E*,19*Z*-docosahexaenoic acid (11,17S-diHDHA, 2 ± 3%), and 16,17*S*-dihydroxy-4*Z*,7*Z*,10*Z*,12*Z*,14*E*,19*Z*-docosahexaenoic acid (16,17S-diHDHA, 16 ± 3%) (Figure S2). PDX was characterized by comparing its retention time and MS fragmentation to those of a PDX standard (*m*/*z* 359.2, 341.21, 323.20, 315.23, 297.22, 290.15, 279.21, 272.14, 261.15, 243.14, 227.14, 206.13, 199.15, 188.12, 181.10, 177.13, 159.12, 153.09, 137.06, and 107.09) and found to be identical (Figures S4 and S5). In addition, the UV spectrum of PDX showed a broad disymmetric triplet, with maximum absorption at 269 nm and shoulders at 259 and 280 nm, with the shoulder at 280 nm being slightly less intense than the shoulder at 259 nm, indicating an EZE conjugation and matching the UV pattern of PDX reported previously[30] (Figure S1). 11,17S-diHDHA and 16,17S-diHDHA were characterized by their MS fragmentations and UV absorption spectra. 11,17S-diHDHA was characterized by its MS fragmentation pattern [*m*/*z* 359.22, 341.21, 323.20, 315.23, 297.22, 290.15, 279.21, 272.14, 261.15, 243.14, 227.14, 199.15, 194.09, 193.09, 165.13, 149.10, 147.12, 121.10, and 95.05 (Figure S6)] and a UV_{max} of 238 nm, indicating two conjugated diene moieties separated by two methylene carbons.[25] Because there are no commercial standards for 11,17-diHDHA, the 11,17-diHDHA generated from h12-LOX and 17S-HpDHA was compared to the 11,17-diHDHA generated from soybean LOX-1 and 11(R/S)-HDHA (Cayman Chemicals) and their retention times, UV spectra, and MS spectra were comparable (Figure S7). 16,17S-diHDHA was characterized by its MS fragmentation pattern [*m*/*z* 359.2, 297.22, 279.21, 272.14, 261.15, 243.14, 231.14,

217.16, 199.15, and 187.12 (Figure S8)] and a UV_{max} of 270 nm, indicating one conjugated triene. It should be noted that because there are no commercially available standards for 11,17S-diHDHA and 16,17S-diHDHA, we cannot confirm the stereochemistry of these products, but because they are oxygenation products, it is appropriate to assume their configurations are 11S,17S-diHDHA and 16R,17S-diHDHA, as has been seen previously for similar dioxygenated LOX products.[18,21]

For h15-LOX-2, there was no observable reaction with either 17S-HpDHA (Table 4) or 17S-HDHA (Table 5). These results reinforce the selective reactivity of h15-LOX-2 to abstract predominately from the ω-8 carbon to produce the ω-6 oxygenation product, which is unavailable with these 17-oxylipin substrates.

The mechanism of these products can be explained as follows. For the generation of the major product, 16S,17S-epoxyDHA, 17S-HpDHA enters the active site methyl end first and h15-LOX-1 abstracts a hydrogen atom from C12 (ω-11), leading to dehydration and epoxide formation. For 16,17S-diHpDHA, the mechanism is the same as for 16S,17S-epoxyDHA; however, in this case, oxygen attacks the radical on C16. Normally, h15-LOX-1 would oxygenate on C17, as it does with DHA, but because C17 is already oxygenated, C16 is the closest carbon for attack. For the other oxygenation product, 11,17S-diHpDHA, it is most likely formed with a methyl end first entry by 17S-HpDHA, followed by abstraction of a hydrogen from C9 (ω-14) and subsequent oxygenation on C11, as seen with DHA in Table 1. PDX, however, cannot be explained by this mechanism because the radical generated by a C9 activation cannot resonate onto C10 with a methyl end first substrate binding. To produce PDX, our hypothesis is that 17S-HpDHA enters the active site with the carboxylate end first, positioning C12 for hydrogen atom abstraction and oxygenation on C10. This is a reasonable assumption because C12 is the "ω-13" position from the carboxylate end, if the oxygen atom is included. This is consistent with previous work, which demonstrated that the methyl end first binding favors a +2 radical rearrangement, while the carboxyl end first favors a −2 radical rearrangement.[31,32] With the proposed carboxylate end first entry binding mode for the production of PDX, it is reasonable to suppose that a negatively charged carboxylate on the substrate would retard entry into the hydrophobic cavity, as observed previously with 14S-HpDHA.[18] To test this hypothesis, we examined PDX production with h15-LOX-1 and 17S-HpDHA under various pH conditions and observed a decrease in the level of PDX production under basic conditions (Figure S9), which supports the hypothesis that deprotonation of the carboxylic acid at high pH inhibits carboxyl end first binding in the active site. It should be noted that fatty acids are known to have high pK_a values, with both LA and DHA having approximate pK_a values from 7 to 8;[33–35] however, the oxylipins will presumably have lower pK_a values due to the disruption of the detergent effect.

The reduced oxylipin, 17S-HDHA, was next reacted with h15-LOX-1, but only the oxygenation product, 16,17S-diHDHA, was observed (Table 5), which is predicted to be in the 16R,17S configuration, on the basis of previous work with 15S-HETE products.[36,37] This is consistent with the fact that the hydroperoxide of 17S-HpDHA is essential for producing the epoxide intermediate for NPD1 biosynthesis, 16S,17S-epoxyDHA. Amazingly, PDX was not detected in the reaction of h15-LOX-1 with 17S-HDHA,

suggesting that the decreased size and hydrophobicity of the C17 alcohol inhibit either the carboxylate end first binding mode or the oxygenation of C10.

With regard to the kinetics of h15-LOX-1 with 17S-HpDHA, the k_{cat}/K_M for the reaction was found to be 0.75 ± 0.2 s^{-1} μM^{-1} and the k_{cat} was found to be 1.8 ± 0.1 s^{-1}, values that were comparable to those of DHA (Table 6A). These results are noteworthy because the hydrogen on 17S-HpDHA that is abstracted is from C12 (ω-11). This is the minority site for hydrogen abstraction for DHA, producing 14S-HpDHA, suggesting a distinct active site binding pose for 17S-HpDHA relative to DHA in the h15-LOX-1 active site. Furthermore, the kinetic parameters of 17S-HDHA were dramatically reduced compared to those of 17S-HpDHA, which could be due to either the need for activation with an oxylipin, as seen with 15S-HETE,[38] or the fact that the epoxidation reaction is the primary reaction mechanism.

In summary, while the kinetic values between DHA and 17S-HpDHA are comparable for h15-LOX-1, they are not similar for h15-LOX-2 and h12-LOX. h15-LOX-2 does not react with 17S-HpDHA, and the kinetic values of h12-LOX are dramatically reduced for 17S-HpDHA, 74-fold lower for k_{cat} and 705-fold lower for k_{cat}/K_M compared to using DHA as the substrate. These data indicate that h15-LOX-1 can accommodate the oxylipin for catalysis better that both h15-LOX-2 and h12-LOX. Interestingly, soybean 15-LOX does not accommodate oxylipins well, with a 470-fold lower k_{cat}/K_M for 15-HpETE relative to AA.[31]

Product Profile and Steady-State Kinetics of h12-LOX with 17S-HpDHA and 17S-HDHA.

h12-LOX was reacted with 17S-HpDHA to determine its ability to produce the NPD1 intermediate, 16S,17S-epoxyDHA, and PDX. The major product under reducing conditions was the oxygenation product 11,17S-diHDHA (52 ± 1%) and two other minor oxygenation products, PDX (22 ± 1%) and 16,17S-diHDHA (5 ± 1%). 10R/S,17S-EEE-diHDHA (21 ± 1%) was also detected as the non-enzymatic hydrolysis products of 16S,17S-epoxyDHA (Table 4 and Figure S2), as seen previously.[17] To confirm these reaction products, h12-LOX was reacted with 17S-HDHA, and as seen for h15-LOX-1, only oxygenation products were observed, 11,17S-diHDHA (73 ± 2%), 16,17S-diHDHA (23 ± 2%), and PDX (4 ± 2%) (Table 5). These observations are consistent with the reaction of h15-LOX-1 with 17S-HDHA, confirming that the lack of the hydroperoxide moiety prohibits epoxidation and thus only oxygenation products are detected.

The kinetics of h12-LOX with 17S-HpDHA was dramatically slower than that of h15-LOX-1 with 17S-HpDHA, with the k_{cat}/K_M being 0.017 ± 0.002 s^{-1} μM^{-1} and the k_{cat} being 0.19 ± 0.01 s^{-1} (Table 6B), which are 45- and 10-fold slower, respectively, than those of the h15-LOX-1 reaction. These data indicate that for h12-LOX, 17S-HpDHA is a worse substrate, relative to h15-LOX-1. This difference is significant because the hydrogen atom abstraction step for both LOX isozymes is from C12 (ω-11) on 17S-HpDHA, which is the preferable hydrogen abstraction position seen for h12-LOX when DHA is the substrate (Table 1). The kinetic parameters of h12-LOX with the reduced substrate, 17S-HDHA, were found to be half as efficient as with 17-HpDHA, most likely due to the loss of the epoxide-generating pathway (Table 6B).

Effective k_{cat}/K_M of 16S,17S-EpoxyDHA and PDX from the Catalysis of h15-LOX-1 and h12-LOX with 17S HpDHA and 17S-HDHA.

Upon comparison of the effective k_{cat}/K_M (i.e., k_{cat}/K_M × percent product) of 16S,17S-epoxyDHA by both h15-LOX-1 and h12-LOX with 17S-HpDHA as the substrate, it was observed that h15-LOX-1 is 55 times more efficient than h12-LOX in producing 16S,17S-epoxyDHA, the precursor of NPD1 (Table 7). We also compared the effective k_{cat}/K_M for PDX by h12-LOX and h15-LOX-1 with 17S-HpDHA as the substrate and determined that h15-LOX-1 is 27 times more efficient than h12-LOX (Table 8). From these results, it is apparent that h15-LOX-1 is more efficient in making the NPD1 intermediate, 16S,17S-epoxyDHA, and PDX than h12-LOX *in vitro*, suggesting that h15-LOX-1 may participate significantly in the formation of NPD1 and PDX *in vivo*.

Allosteric Regulation of 17S-HpDHA and h15-LOX-1 Epoxidation.

The reaction of h15-LOX-1 with 17S-HpDHA (10 μM) favors the epoxidation pathway; however, it was observed that this percentage increased with a decrease in 17S-HpDHA concentration (1 μM), resulting in the formation of non-enzymatic epoxide hydrolysis product 10R/S,17S-EEE-diHDHA as the major product (93 ± 1%). However, at a high 17S-HpDHA concentration (50 μM), the oxygenation pathway was dominant, producing 67 ± 1% oxygenation products (Figure 2). This substantial switch from epoxidation to oxygenation, with an approximately 70% increase in the level of oxygenation products, suggests a possible allosteric regulation, as previously observed with 14S-HpDHA.[18] Furthermore, when the data were fit to a hyperbolic curve, a K_D value of 5.9 ± 1.6 μM was determined, which is similar to the values of previous allosteric regulators that also decreased the level of epoxide production.[18]

This hypothesis was studied further with previously reported allosteric modulators, 12S-HETE and 17S-HDTA, which were titrated into the reaction mixture of h15-LOX-1 and 17S-HpDHA (1 μM), and the epoxidation/oxygenation ratio of 17S-HpDHA was recorded. It should be noted that 12S-HETE and 17S-HDTA were selected as allosteric regulators of h15-LOX-1 because they have minimal reactivity with h15-LOX-1. 12S-HETE titration, from 0 to 25 μM, decreased the level of epoxide production from 93 ± 1% to 30 ± 1%, which resulted in a K_D value of 2.5 ± 0.8 μM. A titration of 17S-HDTA also decreased the level of the epoxidation product, from 93 ± 1% to 51 ± 1%, with a K_D value of 1.4 ± 0.5 μM (Figure 2). Taken together, we conclude that these oxylipins bind to the previously identified allosteric site of h15-LOX-1,[18,27] regulating the epoxidation/oxygenation ratio of 17S-HpDHA. It should be noted that these experiments could not be performed with h12-LOX due to its limited reactivity.

Docking of 17S-HpDHA to h12-LOX and h15-LOX-1.

As we mentioned above, h15-LOX-1 is more efficient than h12-LOX in reacting with 17S-HpDHA in the *in vitro* experiments. To gain a better understanding of this result, computational docking was performed to predict the mode of binding of 17S-HpDHA to the active site of h15-LOX-1 and h12-LOX. First, 17S-HpDHA was docked into h15-LOX-1 with the lowest-energy docking pose being the methyl end first entry pose (Figure 3A). The carboxylate of 17S-HpDHA hydrogen bonds with Arg402, and its aliphatic tail inserts

deep in the hydrophobic pocket created by residues Phe352, Phe414, Ile417, Met418, and Cys559. The hydroperoxide group on C17 hydrogen bonds with residues Glu356 and Gln547. These interactions help position the reactive C12 close (4.5 Å) to the oxygen atom of the hydroxide ion.

Next, we docked the unprotonated 17S-HpDHA into the active site of h12-LOX with the lowest-energy docking pose being the methyl end first entry pose (Figure 3C). The hydroperoxide hydrogen atom of 17S-HpDHA hydrogen bonds with Glu356, while the carboxylate hydrogen bonds with residues Arg402 and Gln406. From this lowest-energy docking pose, we observed that the reactive C12 was located farther from the oxygen atom of hydroxide ion than that seen for h15-LOX-1 (5.5 Å). The larger distance between the reacting centers for h12-LOX than for h15-LOX-1 is consistent with the decreased reactivity of h12-LOX compared to that of h15-LOX-1.

Molecular docking of 17S-HpDHA to h15-LOX-1 and h12-LOX also supports the hypothesis that the production of PDX occurs through protonated carboxylate end first entry, as observed with the decreased level of production of PDX at high pH. 17S-HpDHA was docked into h15-LOX-1 with the protonated carboxylic acid first entry (Figure 3B). The proton of the carboxylic acid of 17S-HpDHA does not form a hydrogen bond with any residue. However, the hydrogen atom of the hydroperoxide moiety makes a hydrogen bond with the C-terminus of residue Ile662. The reactive C12 is 4.1 Å from the oxygen of the hydroxide ion, in this binding pose, which is similar to the distance seen for the methyl end first entry docking pose and suggests that this “flipped” docking pose is catalytically viable.

The protonated form of 17S-HpDHA was also docked into h12-LOX with carboxylic acid first entry (Figure 3D). The carboxylate hydrogen does not hydrogen bond with any active site residue, but the hydrogen of the hydroperoxide group hydrogen bonds with the iron-bound hydroxide ion via the oxygen. The reactive C12 is 7.5 Å from the oxygen atom of the hydroxide ion, supporting the observation that h15-LOX-1 is >27 times more efficient than h12-LOX in producing PDX from 17S-HpDHA.

Metabolites of 17S-HpDHA Obtained after *Ex vivo* Incubations with Human Platelets.

Human platelets have been shown to contain a large amount of h12-LOX, which can produce a great variety of oxylipins when fatty acids in the platelet membrane are cleaved from the phospholipid by phospholipase A2.[26] Considering that h12-LOX is capable of producing the NPD1 intermediate *in vitro* (Table 4), 17S-HpDHA was added to human platelets to determine if metabolite ratios comparable to the *in vitro* measurements were observed. Human platelets treated with 17S-HpDHA (3 μM or 1080 ng/1 × 10^9 platelets) produced only 0.5% dioxylipins, with the primary metabolite being the hydrolysis product of 16S,17S-epoxyDHA (3.7 ng/1 × 10^9 platelets, 75 ± 4% of the total dioxylipins produced) and the minor metabolite being PDX (1.2 ng/1 × 10^9 platelets, 25 ± 4% of the total dioxylipins produced). The observed percentage of PDX production in platelets is similar to that observed *in vitro* (22 ± 1%), but surprisingly, there was no production of 11,17S-diHDHA in platelets, which was shown to be the major metabolite *in vitro* (52 ± 1%). The lack of production of the 11-oxygenation product from 17S-HpDHA (i.e., 11,17S-diHDHA) in platelets could be explained from previous work in which incubation

of human platelets with DHA made vanishingly small amounts of the 11-product (94:6 14S-HDHA:11S-HDHA) compared to the *in vitro* results (81:19 4S-HDHA:11S-HDHA).[18] The major metabolite produced in platelets was the hydrolysis product of 16S,17S-epoxyDHA (75 ± 4%). It should be noted that we assume that much of the 17S-HpDHA added to the platelets is reduced to the alcohol, but detection of the hydrolysis product of 16S,17S-epoxyDHA confirms the hydroperoxide enters the platelet because 16S,17S-epoxyDHA can be produced only starting with the hydroperoxide oxylipin.

The overall amount of oxylipin products produced with 17S-HpDHA in platelets is small. With the addition of 17S-HpDHA (1080 ng total), only 3.7 ng of 16S,17S-epoxyDHA and 1.2 ng of PDX were produced per 1×10^9 platelets, which is <1% of the total 17S-HpDHA that was presented to the platelets. This observation was seen previously upon incubation of 14S-HpDHA with human platelets[18] and is consistent with its poor *in vitro* activity, indicating that 17S-HpDHA is a poor substrate for h12-LOX *ex vivo*.

Effect of 17S-HpDHA, PDX, and 10R/S,17S-EEE-diHDHA on Human Platelet Aggregation.

To determine whether these oxylipins can inhibit human platelet activation, isolated human platelets from five different donors were titrated with 17S-HpDHA, PDX, and 10R/S,17S-EEE-diHDHA (1–10 μM) for 10 min and then stimulated with collagen (0.25 μg/mL). Dimethyl sulfoxide was used as the vehicle control (represented as 0 μM), and 12S-HETrE was chosen as the positive control for comparison.[26] Compared to the vehicle control, 17S-HpDHA inhibited platelet aggregation in response to collagen stimulation with an EC_{50} of <1 μM and had a >90% reduction in platelet aggregation at a concentration of ≥3 μM (Figure 4). This response is significantly more potent than that observed for 12S-HETrE[26] but comparable to that of 11S-HDPA$_{n-6}$ and 14S-HDPA$_{n-6}$[39] (EC_{50} < 1 μM), indicating that 17S-HpDHA is a potent anti-aggregation molecule. The antiplatelet effects of the dihydroxylated oxylipins, PDX and 10R/S,17S-EEE-diHDHA, were also investigated. PDX showed antiplatelet activity with an EC_{50} at low micromolar concentrations (from 1 to 3 μM) and a >90% reduction at a concentration of ≥5 μM, comparable to previous work.[12] However, 10R/S,17S-EEE-diHDHA was markedly less potent, with an EC_{50} of >5 μM, with a 90% reduction at ≥15 μM. This result was consistent with the observation that poxytrins, dihydroxylated fatty acids with an EZE-conjugated triene motif, were potent human platelet aggregation inhibitors (approximately 60% inhibition at 1 μM); however, dihydroxylated fatty acids with an EEE-conjugated triene motif were less potent (approximately 5% inhibition at 1 μM).[40]

DISCUSSION

Neuroprotectin D1 (NPD1) is classified as a specialized pro-resolving mediator (SPM), on the basis of its potent anti-inflammatory activity and pro-resolving action.[41] It has been shown to inhibit polymorphonuclear leukocyte infiltration and macrophage efferocytosis.[8,42] PDX is less potent than NPD1 in resolving inflammation, but it does inhibit collagen-induced platelet aggregation at submicromolar concentrations.[40] For the biosynthesis of these two molecules, it was observed that h15-LOX-1 was involved in the biosynthesis of NPD1 in human macrophage through the 16S,17S-epoxyDHA intermediate;[17] however, no

human LOX isozymes have yet been identified in the biosynthesis of PDX. Only soybean 15-LOX has been identified as a lipoxygenase that could carry out its production.[12] To gain further information about the biosynthesis of NPD1 and PDX, *in vitro* investigations were performed to determine potential routes of their *in vivo* biosynthesis.

In this work, we first investigated which human lipoxygenases were capable of generating the precursor of NPD1 and PDX, 17S-HpDHA. We determined that h12-LOX was slightly more efficient in producing 17S-HpDHA than h15-LOX-1 and h15-LOX-2 from DHA. The effective k_{cat}/K_M of h12-LOX was 2.8-fold greater than that of h15-LOX-1 and 1.3-fold greater than that of h15-LOX-2 (Table 3). This result is surprising because the canonical mechanism of both h15-LOX-1 and h15-LOX-2 is to produce mainly 17S-HpDHA from DHA, while h12-LOX produces primarily 14S-HpDHA as the major product. However, if we take rates into account in the case of DHA as the substrate, k_{cat}/K_M for h12-LOX is greater than those for 15-LOX-1 (34-fold) and h15-LOX-2 (28-fold), resulting in increasing its effective k_{cat}/K_M relative to both h15-LOX isozymes, even though 17S-HpDHA is a minor product for h12-LOX. The other observation that is noteworthy is that the increased percentage of the ω-9 product with DHA relative to AA (i.e., ω-11 hydrogen abstraction) indicates that the increased length and degree of unsaturation allow DHA to insert deeper into the h15-LOX-1 and h15-LOX-2 active sites, as previously observed.[18] This increased reactivity of h15-LOX-1 and h15-LOX-2 with DHA made us suspect that they might be capable of contributing to the next step of NPD1 and PDX biosynthesis, which requires an ω-11 hydrogen abstraction.

Utilizing 17S-HpDHA as the substrate, it was determined that both h15-LOX-1 and h12-LOX were capable of producing 16S,17S-epoxyDHA, indicating that both of these lipoxygenases abstract a hydrogen atom from C12 (ω-11) of 17S-HpDHA. However, h15-LOX-1 is 44-fold more kinetically efficient (i.e., k_{cat}/K_M) with 17S-HpDHA than h12-LOX. This result is significant because the ω-11 carbon is the preferable hydrogen abstraction position for h12-LOX, yet the reaction is slower than expected with the oxylipin. This decreased rate of catalysis for h12-LOX with oxylipins was previously observed for 14S-HpDHA, indicating the active site for h12-LOX is more restrictive with respect to the substrate structure.[18] We also investigated if h15-LOX-2 could be responsible for the biosynthesis of 16S,17S-epoxyDHA, because it was observed to abstract from the ω-11 carbon and produce the ω-9 product, 14S-HpHDHA, from DHA. Surprisingly, no reaction was observed for h15-LOX-2 with 17S-HpDHA or the reduced substrate, 17S-HDHA. This lack of reactivity is also consistent with previous work in which h15-LOX-2 did not react with 14S-HpDHA,[18] indicating the active site of h15-LOX-2 is also selective against oxylipins, similar to h12-LOX.

When the reduced form of 17S-HpDHA, 17S-HDHA, was reacted with h15-LOX-1 and h12-LOX, it was confirmed that the lack of the hydroperoxide moiety prohibited the dehydration reaction to make the epoxide. Thus, only the oxygenation products, 16,17S-diHDHA for h15-LOX-1 and 11,17S-diHDHA, 16,17S-diHDHA, and PDX for h12-LOX, were detected under reducing condition. These results build on previous work,[16,18] where the chemical nature of the oxylipin is critical to the biosynthesis of lipoxins, maresins, and NPD1, to name a few, which all require an epoxide intermediate. However, if the

hydroperoxide precursor is reduced by glutathione peroxidases 4 (GPx4) in the cell, then the level of biosynthesis of these critical SPMs will be greatly diminished, indicating the importance of GPx4 and glutathione concentrations in the inflammatory response. Unexpectedly, the oxygenation product, PDX, is also affected by the nature of the oxylipin substrate. PDX was not detected in the reaction of 17S-HDHA with h15-LOX-1 and was barely detected in the reaction with h12-LOX (4%), suggesting that the synthetic route for PDX is initiated by 17S-HpDHA as the substrate, not the reduced form, as was suggested in the literature.[30]

Although both h15-LOX-1 and h12-LOX react with 17S-HpDHA to produce 16S,17S-epoxyDHA and PDX, the efficiency is not comparable. It was observed that the effective k_{cat}/K_M of h15-LOX-1 (k_{cat}/K_M × percent product) is 55 times more efficient than that of h12-LOX in producing 16S,17S-epoxyDHA and >27 times more efficient in generating PDX (Table 7), implying that h15-LOX-1 may contribute more than h12-LOX to NPD1 and PDX formation *in vivo*. This is supported by the fact that a significant reduction in NPD1 and PDX production was observed with h15-LOX-1 deficient mice, compared to the wild type.[43] Furthermore, the role of h15-LOX-1 in NPD1 and PDX biosynthesis was further corroborated by the challenge of the h15-LOX-1 inhibitor, PD146176, to M2 macrophages, resulting in the decrease in the levels of NPD1 and PDX production by 32% and 29%, respectively.[43] Despite the low efficiency of 16S,17S-epoxyDHA and PDX production in the reaction of 17S-HpDHA with h12-LOX *in vitro*, a different outcome is possible *in vivo*. Therefore, the production of NPD1 and PDX was monitored with the incubation of 17S-HpDHA with human platelets that contain large quantities of h12-LOX. Our results suggest that the primary metabolite of 17S-HpDHA with human platelets is the epoxidation product, 16S,17S-epoxyDHA (75 ± 4%), with a minor production of PDX (25 ± 4%). However, the overall turnover number of 17S-HpDHA by platelets *ex vivo* is low (0.5% converted to the dioxylipin), indicating that this pathway may not be important *in vivo*.

A proposed biosynthetic scheme of NPD1 and PDX from h12-LOX and h15-LOX-1 is presented in Scheme 1, with the size of the arrows representing the magnitude of their effective k_{cat}/K_M. It should be noted that the *in vitro* biosynthetic flux values may vary from the *in vivo* results because in the cell there are many variables that could affect these rates, such as protein expression or protein–protein interactions, as seen with 5-LOX-activating protein (FLAP), which can facilitate AA conversion with h5-LOX.[44]

As mentioned in the introductory section, NPD1 displays anti-inflammatory and pro-resolving properties during inflammation, while PDX shows more antiplatelet aggregation activity instead of inflammatory resolution. Therefore, a change in the NPD1:PDX ratio in the cell could affect the inflammatory response. Previously, we determined that the epoxide:oxygenated product ratio of 14S-HpDHA with h15-LOX-1 was affected by allosteric effectors, such as 14S-HpDHA. In this work, similar results were revealed with increasing concentrations of 17S-HpDHA, where the level of production of the NPD1 intermediate, 16S,17S-epoxyDHA, decreased and that of PDX increased, thus indicating a product-feedback loop for NPD1 and PDX formation. These data suggest that allosteric effectors could change the NPD1:PDX ratio *in vivo*, and we are currently investigating if LOX products can regulate this ratio and establish a product-feedback loop in the cell.

The mono- and dihydroxylated DHA-derived oxylipins were then examined to determine their ability to inhibit collagen-induced platelet aggregation. Our findings indicated that 17S-HpDHA was active with respect to platelet aggregation inhibition, with an EC_{50} of <1 μM. This response is comparable to the effect observed for 14S-HpDHA,[18] 11S-$HDPA_{n-6}$, and 14S-$HDPA_{n-6}$ oxylipins,[39] but significantly more potent than 12S-HETrE.[26] For the dihydroxylated oxylipins, we observed that PDX showed antiplatelet activity with an EC_{50} of low-micromolar values (from 1 to 3 μM). However, 10R/S,17S-EEE-diHDHA, the non-enzymatic hydrolysis product of 16S,17S-epoxyDHA, was markedly less potent, with an EC_{50} of >5 μM. These values of 17S-HpDHA platelet potency could affect platelet biology, because its biological concentrations are comparable to its platelet potency.[45,46] However, the biologically detected concentrations of PDX and 10R/S,17S-EEE-diHDHA are markedly less than that of their platelet response, indicating they may not be relevant for platelet activation.[47,48]

CONCLUSION

In summary, we have shown that while h12-LOX and h15-LOX-1 are both viable enzymes for the production of the NPD1 epoxide intermediate and PDX, h15-LOX-1 is a more efficient pathway to their *in vitro* biosynthesis by >55- and >27-fold, respectively. Moreover, we have demonstrated the allosteric regulation of NPD1 and PDX biosynthesis for h15-LOX-1 by oxylipins can negatively regulate NPD1 epoxide intermediate production. Given that 17S-HpDHA and 12S-HETE have micromolar potency for affecting the NPD1:PDX ratio *in vitro*, it is biologically feasible that NPD1 and PDX concentrations could be affected by oxylipins in the cell, which is in agreement with previous work.[18] Lastly, 17S-HpDHA is a potent antiplatelet metabolite of DHA, indicating an additional dietary benefit for fish oil consumption. These new conclusions regarding the biochemistry of NPD1 and PDX will help direct inhibitor development and possibly guide *in vivo* biosynthetic investigations.

Supplementary Material

Refer to Web version on PubMed Central for supplementary material.

Funding

National Institutes of Health Grants R01 GM105671 (M.H. and T.R.H.), R01 HL11405 (M.H. and T.R.H.), and R35 GM131835 (M.H. and T.R.H.).

ABBREVIATIONS

DHA	docosahexaenoic acid
DTA	docosatrienoic acid
AA	arachidonic acid
17S-HpDHA	17*S*-hydroperoxy-4*Z*,7*Z*,10*Z*,13*Z*,15*E*,19*Z*-docosahexaenoic acid

17S-HDHA	17*S*-hydroxy-4*Z*,7*Z*,10*Z*,13*Z*,15*E*,9*Z*-docosahexaenoic acid
16S,17S-epoxyDHA	16*S*,17*S*-epoxy-4*Z*,7*Z*,10*Z*,12*E*,14*E*,19*Z*-docosahexaenoic acid
10R/S,17S-EEE-diHDHA	10*R*/*S*,17*S*-dihydroxy-4*Z*,7*Z*,11*E*,13*E*,15*E*,19*Z*-docosahexaenoic acid
11,17S-diHDHA	11,17*S*-dihydroxy-4*Z*,7*Z*,9*E*,13*Z*,15*E*,19*Z*-docosahexaenoic acid
16,17S-diHDHA	16,17*S*-dihydroxy-4*Z*,7*Z*,10*Z*,12*Z*,14*E*,19*Z*-docosahexaenoic acid
15S-HpETE	15*S*-hydroperoxy-5*Z*,8*Z*,11*Z*,13*E*-eicosatetraenoic acid
12S-HETrE	12*S*-hydroxy-8*Z*,10*E*,14*Z*-eicosatrienoic acid
12S-HETE	12*S*-hydroxy-5*Z*,8*Z*,10*E*,14*Z*-eicosatetraenoic acid
17S-HDTA	17*S*-hydroxy-13*Z*,15*E*,19*Z*-docosatrienoic acid
PDX	protectin DX
NPD1	neuroprotectin D1 [also known as protectin D1 (PD1)]
PCTRs	protectin conjugates in tissue regeneration
MCTRs	maresin conjugates in tissue regeneration
LXs	AA-derived lipoxins
RvEs	EPA-derived E-series resolvins
RvDs	DHA-derived D-series resolvins
RvTs	DPA-derived 13-series resolvins
LXB_4	lipoxin B4
SPM	specialized pro-resolving mediator
PUFA	polyunsaturated fatty acid
ROS	reactive oxygen species
AD	Alzheimer’s disease
ALS	amyotrophic lateral sclerosis
NSAIDs	nonsteroidal anti-inflammatory drugs
BIR	brain ischemia reperfusion
RPE	retina pigment epithelial

ICP-MS	inductively coupled plasma mass spectrometry
CAD	collisionally activated dissociation
COX	cyclooxygenase
LOX	lipoxygenase
h15-LOX-1 (ALOX15)	human reticulocyte 15-lipoxygenase-1
h12-LOX (ALOX12)	human platelet 12-lipoxygenase
h15-LOX-2 (ALOX15B)	human epithelial 15-lipoxygenase-2
sLOX-1	soybean lipoxygenase-1

REFERENCES

(1). Chen L, Deng H, Cui H, Fang J, Zuo Z, Deng J, Li Y, Wang X, and Zhao L (2018) Inflammatory responses and inflammation-associated diseases in organs. Oncotarget 9, 7204–7218. [PubMed: 29467962]

(2). Tabas I, and Glass CK (2013) Anti-inflammatory therapy in chronic disease: challenges and opportunities. Science 339, 166–172. [PubMed: 23307734]

(3). Chiurchiù V, Leuti A, and Maccarrone M (2018) Bioactive Lipids and Chronic Inflammation: Managing the Fire Within. Front. Immunol 9, 38. [PubMed: 29434586]

(4). Wongrakpanich S, Wongrakpanich A, Melhado K, and Rangaswami J (2018) A Comprehensive Review of Non-Steroidal Anti-Inflammatory Drug Use in The Elderly. Aging Dis 9, 143–150. [PubMed: 29392089]

(5). Serhan CN, Chiang N, and Van Dyke TE (2008) Resolving inflammation: dual anti-inflammatory and pro-resolution lipid mediators. Nat. Rev. Immunol 8, 349–361. [PubMed: 18437155]

(6). Sugimoto MA, Sousa LP, Pinho V, Perretti M, and Teixeira MM (2016) Resolution of Inflammation: What Controls Its Onset? Front. Immunol 7, 160. [PubMed: 27199985]

(7). Wisastra R, and Dekker FJ (2014) Inflammation, Cancer and Oxidative Lipoxygenase Activity are Intimately Linked. Cancers 6, 1500–1521. [PubMed: 25037020]

(8). Serhan CN, Gotlinger K, Hong S, Lu Y, Siegelman J, Baer T, Yang R, Colgan SP, and Petasis NA (2006) Anti-inflammatory actions of neuroprotectin D1/protectin D1 and its natural stereoisomers: assignments of dihydroxy-containing docosatrienes. J. Immunol 176, 1848–1859. [PubMed: 16424216]

(9). Bazan NG (2005) Neuroprotectin D1 (NPD1): a DHA-derived mediator that protects brain and retina against cell injury-induced oxidative stress. Brain Pathol 15, 159–166. [PubMed: 15912889]

(10). Bazan NG (2009) Neuroprotectin D1-mediated anti-inflammatory and survival signaling in stroke, retinal degenerations, and Alzheimer's disease. J. Lipid Res 50 (Suppl), S400–405. [PubMed: 19018037]

(11). Butovich IA (2005) On the structure and synthesis of neuroprotectin D1, a novel anti-inflammatory compound of the docosahexaenoic acid family. J. Lipid Res 46, 2311–2314. [PubMed: 16150835]

(12). Chen P, Fenet B, Michaud S, Tomczyk N, Vericel E, Lagarde M, and Guichardant M (2009) Full characterization of PDX, a neuroprotectin/protectin D1 isomer, which inhibits blood platelet aggregation. FEBS Lett 583, 3478–3484. [PubMed: 19818771]

(13). Hong S, Gronert K, Devchand PR, Moussignac RL, and Serhan CN (2003) Novel docosatrienes and 17S-resolvins generated from docosahexaenoic acid in murine brain, human blood, and glial cells. Autacoids in anti-inflammation. J. Biol. Chem 278, 14677–14687. [PubMed: 12590139]

(14). Lagarde M, Guichardant M, and Bernoud-Hubac N (2020) Anti-inflammatory and anti-virus potential of poxytrins, especially protectin DX. Biochimie 179, 281–284. [PubMed: 32956736]

(15). Brash AR (1999) Lipoxygenases: occurrence, functions, catalysis, and acquisition of substrate. J. Biol. Chem 274, 23679–23682. [PubMed: 10446122]

(16). Green AR, Freedman C, Tena J, Tourdot BE, Liu B, Holinstat M, and Holman TR (2018) 5 S,15 S-Dihydroperoxy-eicosatetraenoic Acid (5,15-diHpETE) as a Lipoxin Intermediate: Reactivity and Kinetics with Human Leukocyte 5-Lipoxygenase, Platelet 12-Lipoxygenase, and Reticulocyte 15-Lipoxygenase-1. Biochemistry 57, 6726–6734. [PubMed: 30407793]

(17). Aursnes M, Tungen JE, Colas RA, Vlasakov I, Dalli J, Serhan CN, and Hansen TV (2015) Synthesis of the 16S,17S-Epoxyprotectin Intermediate in the Biosynthesis of Protectins by Human Macrophages. J. Nat. Prod 78, 2924–2931. [PubMed: 26580578]

(18). Freedman C, Tran A, Tourdot BE, Kalyanaraman C, Perry S, Holinstat M, Jacobson MP, and Holman TR (2020) Biosynthesis of the Maresin Intermediate, 13S,14S-Epoxy-DHA, by Human 15-Lipoxygenase and 12-Lipoxygenase and Its Regulation through Negative Allosteric Modulators. Biochemistry 59, 1832–1844. [PubMed: 32324389]

(19). Kutzner L, Goloshchapova K, Heydeck D, Stehling S, Kuhn H, and Schebb NH (2017) Mammalian ALOX15 orthologs exhibit pronounced dual positional specificity with docosahexaenoic acid. Biochim. Biophys. Acta, Mol. Cell Biol. Lipids 1862, 666–675. [PubMed: 28400162]

(20). Perry SC, Horn T, Tourdot BE, Yamaguchi A, Kalyanaraman C, Conrad WS, Akinkugbe O, Holinstat M, Jacobson MP, and Holman TR (2020) Role of Human 15-Lipoxygenase-2 in the Biosynthesis of the Lipoxin Intermediate, 5S,15S-diHpETE, Implicated with the Altered Positional Specificity of Human 15-Lipoxygenase-1. Biochemistry 59, 4118–4130. [PubMed: 33048542]

(21). Perry SC, Kalyanaraman C, Tourdot BE, Conrad WS, Akinkugbe O, Freedman JC, Holinstat M, Jacobson MP, and Holman TR (2020) 15-Lipoxygenase-1 biosynthesis of 7S,14S-diHDHA implicates 15-lipoxygenase-2 in biosynthesis of resolvin D5. J. Lipid Res 61, 1087–1103. [PubMed: 32404334]

(22). Amagata T, Whitman S, Johnson TA, Stessman CC, Loo CP, Lobkovsky E, Clardy J, Crews P, and Holman TR (2003) Exploring sponge-derived terpenoids for their potency and selectivity against 12-human, 15-human, and 15-soybean lipoxygenases. J. Nat. Prod 66, 230–235. [PubMed: 12608855]

(23). Vasquez-Martinez Y, Ohri RV, Kenyon V, Holman TR, and Sepulveda-Boza S (2007) Structure-activity relationship studies of flavonoids as potent inhibitors of human platelet 12-hLO, reticulocyte 15-hLO-1, and prostate epithelial 15-hLO-2. Bioorg. Med. Chem 15, 7408–7425. [PubMed: 17869117]

(24). Butovich IA (2006) A one-step method of 10,17-dihydro(pero)xydocosahexa-4Z,7Z,11E,13Z,15E,19Z-enoic acid synthesis by soybean lipoxygenase. J. Lipid Res 47, 854–863. [PubMed: 16391324]

(25). Jiang ZD, and Gerwick WH (1997) Novel oxylipins from the temperate red alga Polyneura latissima: evidence for an arachidonate 9(S)-lipoxygenase. Lipids 32, 231–235. [PubMed: 9076659]

(26). Ikei KN, Yeung J, Apopa PL, Ceja J, Vesci J, Holman TR, and Holinstat M (2012) Investigations of human platelet-type 12-lipoxygenase: role of lipoxygenase products in platelet activation. J. Lipid Res 53, 2546–2559. [PubMed: 22984144]

(27). Wecksler AT, Kenyon V, Deschamps JD, and Holman TR (2008) Substrate specificity changes for human reticulocyte and epithelial 15-lipoxygenases reveal allosteric product regulation. Biochemistry 47, 7364–7375. [PubMed: 18570379]

(28). Green AR, Barbour S, Horn T, Carlos J, Raskatov JA, and Holman TR (2016) Strict Regiospecificity of Human Epithelial 15-Lipoxygenase-2 Delineates Its Transcellular Synthesis Potential. Biochemistry 55, 2832–2840. [PubMed: 27145229]

(29). Guichardant M, Vericel E, and Lagarde M (2019) Biological relevance of double lipoxygenase products of polyunsaturated fatty acids, especially within blood vessels and brain. Biochimie 159, 55–58. [PubMed: 30179647]

(30). Balas L, Guichardant M, Durand T, and Lagarde M (2014) Confusion between protectin D1 (PD1) and its isomer protectin DX (PDX). An overview on the dihydroxy-docosatrienes described to date. Biochimie 99, 1–7. [PubMed: 24262603]

(31). Van Os CP, Rijke-Schilder GP, Van Halbeek H, Verhagen J, and Vliegenthart JF (1981) Double dioxygenation of arachidonic acid by soybean lipoxygenase-1. Kinetics and regio-stereo specificities of the reaction steps. Biochim. Biophys. Acta, Lipids Lipid Metab 663, 177–193.

(32). Hornung E, Walther M, Kuhn H, and Feussner I (1999) Conversion of cucumber linoleate 13-lipoxygenase to a 9-lipoxygenating species by site-directed mutagenesis. Proc. Natl. Acad. Sci. U. S. A 96, 4192–4197. [PubMed: 10097186]

(33). Bild GS, Ramadoss CS, and Axelrod B (1977) Effect of substrate polarity on the activity of soybean lipoxygenase isoenzymes. Lipids 12, 732–735.

(34). Glickman MH, and Klinman JP (1995) Nature of Rate-Limiting Steps in the Soybean Lipoxygenase-1 Reaction. Biochemistry 34, 14077–14092. [PubMed: 7578005]

(35). Dobson EP, Barrow CJ, Kralovec JA, and Adcock JL (2013) Controlled formation of mono- and dihydroxy-resolvins from EPA and DHA using soybean 15-lipoxygenase. J. Lipid Res 54, 1439–1447. [PubMed: 23471029]

(36). Maas RL, and Brash AR (1983) Evidence for a lipoxygenase mechanism in the biosynthesis of epoxide and dihydroxy leukotrienes from 15(S)-hydroperoxyicosatetraenoic acid by human platelets and porcine leukocytes. Proc. Natl. Acad. Sci. U. S. A 80, 2884–2888. [PubMed: 6304687]

(37). Radmark O, Serhan C, Hamberg M, Lundberg U, Ennis MD, Bundy GL, Oglesby TD, Aristoff PA, Harrison AW, Slomp G, et al. (1984) Stereochemistry, total synthesis, and biological activity of 14,15-dihydroxy-5,8,10,12-eicosatetraenoic acid. J. Biol. Chem 259, 13011–13016. [PubMed: 6092359]

(38). Kuhn H, Wiesner R, Stender H, Schewe T, Lankin VZ, Nekrasov A, and Rapoport SM (1986) Requirement of monohydroperoxy fatty acids for the oxygenation of 15LS-HETE by reticulocyte lipoxygenase. FEBS Lett 203, 247–252. [PubMed: 3089837]

(39). Yeung J, Adili R, Yamaguchi A, Freedman CJ, Chen A, Shami R, Das A, Holman TR, and Holinstat M (2020) Omega-6 DPA and its 12-lipoxygenase-oxidized lipids regulate platelet reactivity in a nongenomic PPARα-dependent manner. Blood Adv 4, 4522–4537. [PubMed: 32946570]

(40). Chen P, Vãricel E, Lagarde M, and Guichardant M (2011) Poxytrins, a class of oxygenated products from polyunsaturated fatty acids, potently inhibit blood platelet aggregation. FASEB J 25, 382–388. [PubMed: 20833872]

(41). Hansen TV, Vik A, and Serhan CN (2019) The Protectin Family of Specialized Pro-resolving Mediators: Potent Immunoresolvents Enabling Innovative Approaches to Target Obesity and Diabetes. Front. Pharmacol 9, 1582. [PubMed: 30705632]

(42). Schwab JM, Chiang N, Arita M, and Serhan CN (2007) Resolvin E1 and protectin D1 activate inflammation-resolution programmes. Nature 447, 869–874. [PubMed: 17568749]

(43). Pistorius K, Souza PR, De Matteis R, Austin-Williams S, Primdahl KG, Vik A, Mazzacuva F, Colas RA, Marques RM, Hansen TV, and Dalli J (2018) PDn-3 DPA Pathway Regulates Human Monocyte Differentiation and Macrophage Function. Cell Chem. Biol 25, 749–760. [PubMed: 29805036]

(44). Gerstmeier J, Newcomer ME, Dennhardt S, Romp E, Fischer J, Werz O, and Garscha U (2016) 5-Lipoxygenase-activating protein rescues activity of 5-lipoxygenase mutations that delay nuclear membrane association and disrupt product formation. FASEB J 30, 1892–1900. [PubMed: 26842853]

(45). Yeung J, Adili R, Yamaguchi A, Freedman CJ, Chen A, Shami R, Das A, Holman TR, and Holinstat M (2020) Omega-6 DPA and its 12-lipoxygenase-oxidized lipids regulate platelet reactivity in a nongenomic PPARalpha-dependent manner. Blood Adv 4, 4522–4537. [PubMed: 32946570]

(46). Fischer R, Konkel A, Mehling H, Blossey K, Gapelyuk A, Wessel N, von Schacky C, Dechend R, Muller DN, Rothe M, Luft FC, Weylandt K, and Schunck WH (2014) Dietary omega-3 fatty

acids modulate the eicosanoid profile in man primarily via the CYP-epoxygenase pathway. J. Lipid Res 55, 1150–1164. [PubMed: 24634501]

(47). Skarke C, Alamuddin N, Lawson JA, Li X, Ferguson JF, Reilly MP, and FitzGerald GA (2015) Bioactive products formed in humans from fish oils. J. Lipid Res 56, 1808–1820. [PubMed: 26180051]

(48). Souza PR, Marques RM, Gomez EA, Colas RA, De Matteis R, Zak A, Patel M, Collier DJ, and Dalli J (2020) Enriched Marine Oil Supplements Increase Peripheral Blood Specialized Pro-Resolving Mediators Concentrations and Reprogram Host Immune Responses: A Randomized Double-Blind Placebo-Controlled Study. Circ. Res 126, 75–90. [PubMed: 31829100]

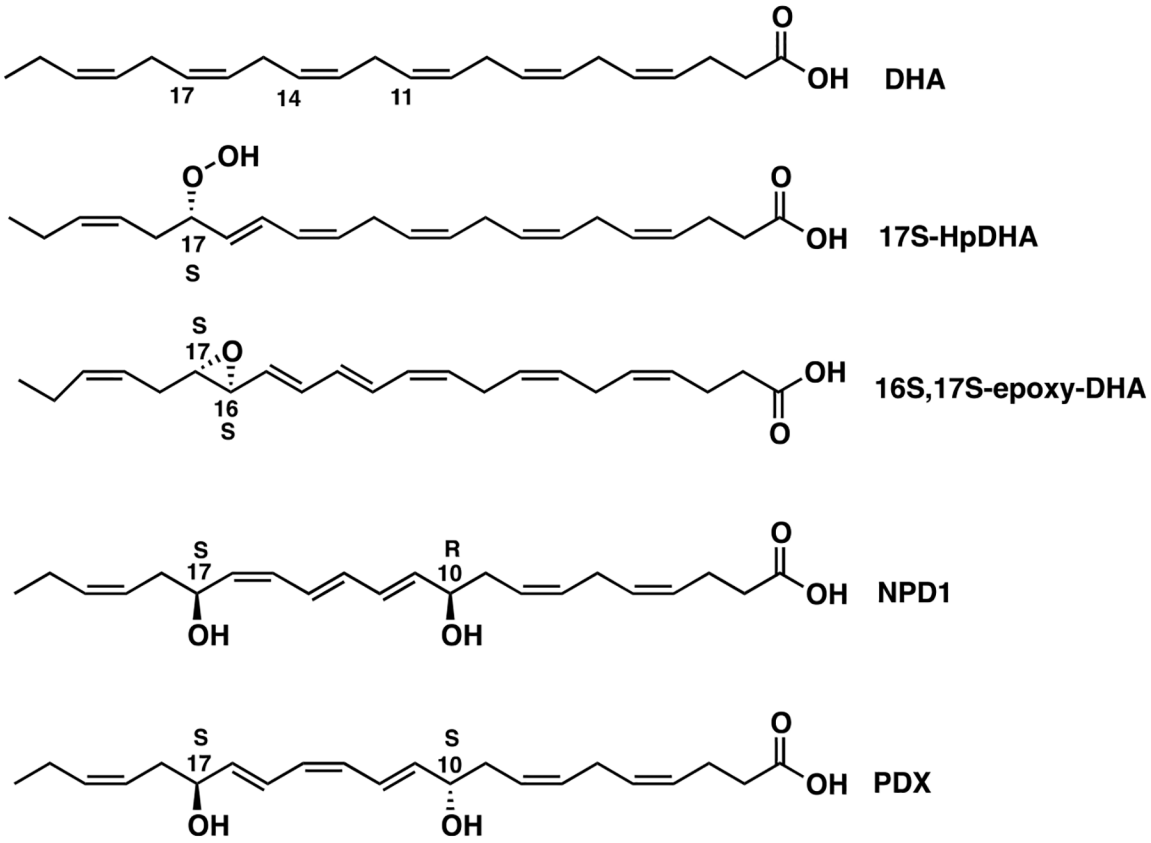

Figure 1.
Structures of DHA, 17S-HpDHA, 16S,17S-epoxyDHA, NPD1, and PDX.

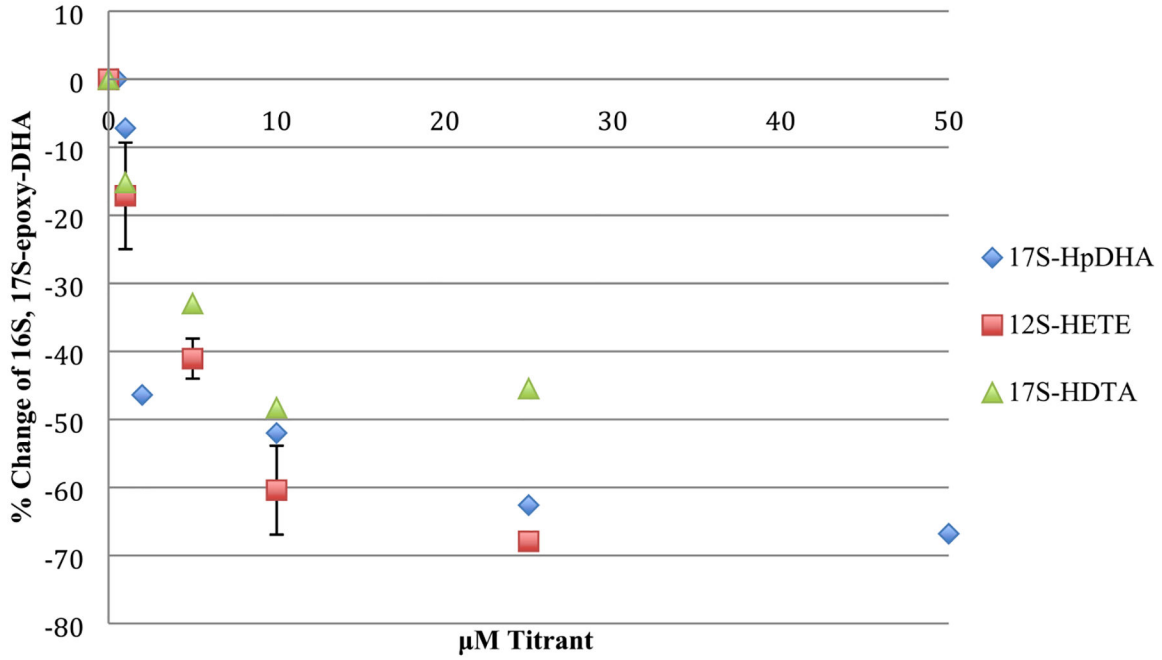

Figure 2.

Percent change in 16S,17S-epoxyDHA through h15-LOX-1 allosteric regulation of 17S-HpDHA epoxidation. h15-LOX-1 reacted with increasing concentrations of 17S-HpDHA (blue diamonds), 17S-HpDHA (1 μM) with increasing concentrations of 12S-HETE (red squares), and 17S-HpDHA (1 μM) with increasing concentrations of 17S-HDTA (green triangles). Note that 1 μM 17S-HpDHA is required for the second two reactions because 12S-HETE and 17S-HDTA are not substrates.

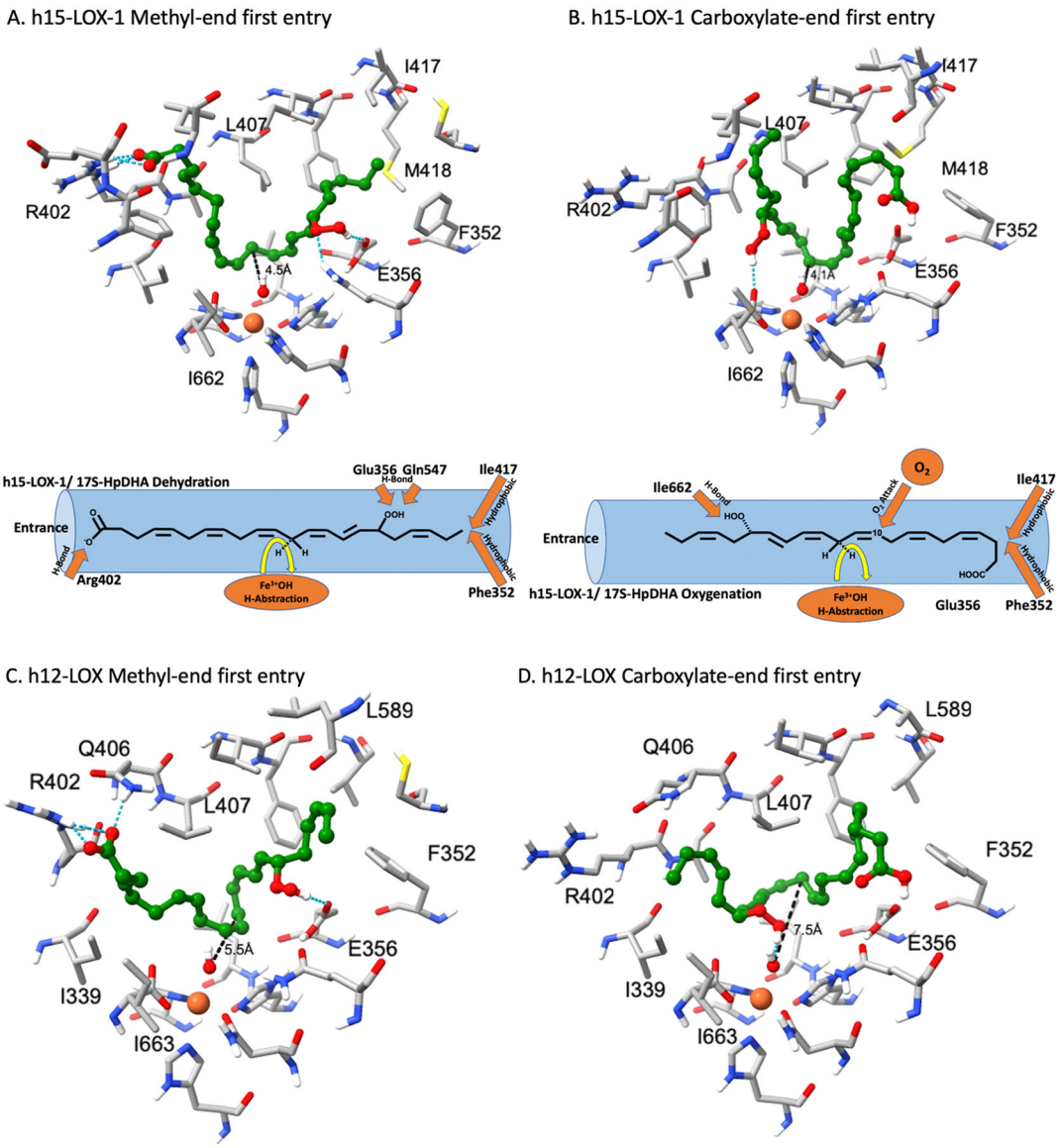

Figure 3.

Docking poses of charged and neutral 17S-HpDHA against h12-LOX and h15-LOX-1. (A) Charged 17S-HpDHA docked to h15-LOX-1. (B) Neutral 17S-HpDHA docked to h15-LOX-1. (C) Charged 17S-HpDHA docked to h12-LOX. (D) Neutral 17S-HpDHA docked to h12-LOX. Carbon atoms of the protein and substrate are colored gray and green, respectively. Nitrogen, oxygen, hydrogen, sulfur, and Fe^{3+} are colored blue, red, white, yellow, and tan, respectively. Residues providing polar and hydrophobic interactions to the substrate are labeled. Distances between the oxygen atom of the hydroxide ion and C12 of the substrate are shown. Hydrogen bonds between the substrate and the protein are colored cyan.

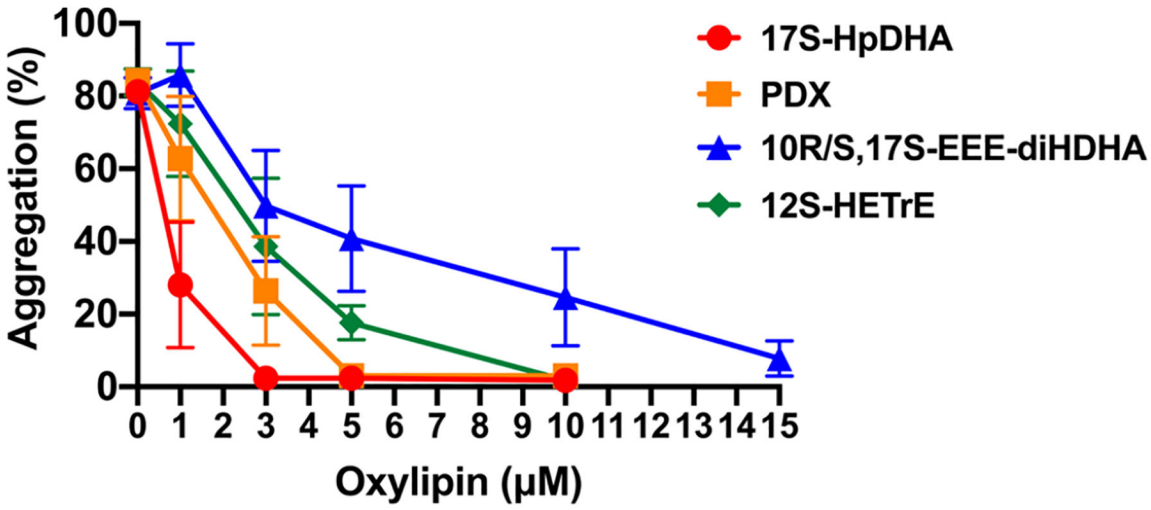

Figure 4.

Inhibition of collagen-stimulated platelet aggregation by 17S-HpDHA, PDX, 10R/S,17S-EEE-diHDHA, and 12S-HETrE. 17S-HpDHA, PDX, and 10R/S,17S-EEE-diHDHA (ranging from 1 to 15 μM) were incubated with isolated human platelets and then stimulated with collagen (0.25 μg/mL). Data represent means ± the standard error of the mean of the maximum aggregation of five independent experiments.

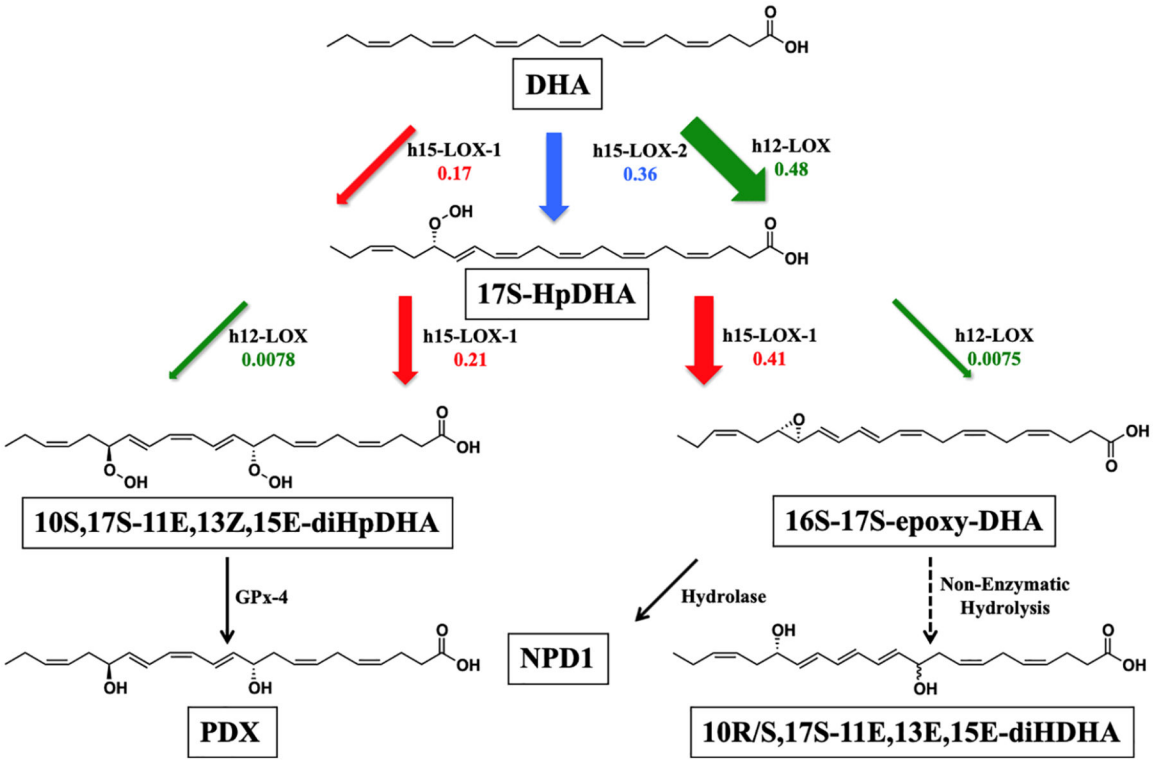

Scheme 1. A Proposed Biosynthetic Scheme of NPD1 and PDX with the Lipoxygenase Isozyme[a]

[a]The size of the arrows is proportional to their effective k_{cat}/K_M (i.e., k_{cat}/K_M × percent product).

Table 1.

Product Profiles of h15-LOX-1, h15-LOX-2, and h12-LOX (percent) upon Reaction with 10 μM DHA

	17S-HpDHA	14S-HpDHA	11S-HpDHA
h15-LOX-1[a]	49 ± 2	37 ± 2	14 ± 2
h15-LOX-2	84 ± 1	16 ± 1	0
h12-LOX	4 ± 1	78 ± 1	18 ± 1

[a]Note that trace amounts of 20S-HpDHA were found to be <3% in the reaction of DHA and h15-LOX-1.

Table 2.

Steady-State Kinetic Parameters for h15-LOX-1, h15-LOX-2, and h12-LOX with AA and DHA[a]

enzyme	substrate	k_{cat} (s^{-1})	K_M (μM)	k_{cat}/K_M ($s^{-1}\ \mu M^{-1}$)	relative k_{cat}/K_M[b]
h15-LOX-1	AA	4.1 ± 0.2	4.2 ± 0.5	0.98 ± 0.1	1.0
h15-LOX-1	DHA	2.3 ± 0.6	6.7 ± 3	0.35 ± 0.08	0.36
h15-LOX-2	AA	2.5 ± 0.3	11 ± 2	0.24 ± 0.02	0.24
h15-LOX-2	DHA	4.2 ± 0.3	9.8 ± 1	0.43 ± 0.03	0.44
h12-LOX	AA	17 ± 0.5	1.2 ± 0.2	14 ± 0.5	14
h12-LOX	DHA	14 ± 0.5	1.2 ± 0.2	12 ± 2	12

[a]The rates of h15-LOX-1, h15-LOX-2, and h12-LOX with AA were consistent with previous values.[26–28]

[b]The relative k_{cat}/K_M values were scaled to the reaction of h15-LOX-1 and AA being set to 1.

Table 3.

Effective k_{cat}/K_M (k_{cat}/K_M × percent product) for the Production of 17S-HpDHA from DHA for h15-LOX-1, h15-LOX-2, and h12-LOX

	17S-HpDHA effective k_{cat}/K_M	relative 17S-HpDHA effective k_{cat}/K_M[a]
h15-LOX-1	0.17	1
h15-LOX-2	0.36	2.1
h12-LOX	0.48	2.8

[a]The relative 17S-HpDHA effective k_{cat}/K_M values were scaled to the reaction of h15-LOX-1 and DHA being set to 1.

Table 4.

Product profile of h12-LOX, h15-LOX-1, and h15-LOX-2 with 2 μM 17S-HpDHA

	11,17S-diHDHA	16S,17S-epoxyDHA[a]	PDX	16,17S-diHDHA
h12-LOX	52 ± 1	21 ± 1	22 ± 1	5 ± 1
h15-LOX-1	2 ± 3	54 ± 3	28 ± 3	16 ± 3
h15-LOX-2	n/r	n/r	n/r	n/r

[a]10R/S,17S-EEE-diHDHA is the detected product from the non-enzymatic hydrolysis of 16S,17S-epoxyDHA. No reaction (n/r) was detectable after the incubation of h15-LOX-2 with 17S-HpDHA.

Table 5.

Product Profile of h12-LOX, h15-LOX-1, and h15-LOX-2 with 2 μM 17S-HDHA[a]

	11,17S-diHDHA	PDX	16,17S-diHDHA
h12-LOX	73 ± 2	4 ± 2	23 ± 2
h15-LOX-1	0	0	100
h15-LOX-2	n/r	n/r	n/r

[a]No reaction (n/r) was detectable after the incubation of h15-LOX-2 with 17S-HDHA.

Table 6.

Steady-State Kinetics of (A) h15-LOX-1 and (B) h12-LOX with DHA, 17S-HpDHA, and 17S-HDHA[a]

(A) h15-LOX-1					
enzyme	**substrate**	**k_{cat} (s^{-1})**	**K_M (μM)**	**k_{cat}/K_M (s^{-1} μM^{-1})**	**relative k_{cat}/K_M[b]**
h15-LOX-1	DHA	2.3 ± 0.6	6.7 ± 3	0.35 ± 0.08	1
h15-LOX-1	17S-HpDHA	1.8 ± 0.1	2.4 ± 0.6	0.75 ± 0.2	2.1
h15-LOX-1	17S-HDHA	0.27 ± 0.02	37 ± 9	0.0070 ± 0.001	0.02
(B) h12-LOX					
enzyme	**substrate**	**k_{cat} (s^{-1})**	**K_M (μM)**	**k_{cat}/K_M (s^{-1} μM^{-1})**	**relative k_{cat}/K_M[b]**
h12-LOX	DHA	14 ± 0.5	1.2 ± 0.2	12 ± 2	1
h12-LOX	17S-HpDHA	0.19 ± 0.01	12 ± 1.9	0.017 ± 0.002	0.0015
h12-LOX	17S-HDHA	0.25 ± 0.02	29 ± 6.3	0.0080 ± 0.001	0.0007

[a]The DHA reactions were monitored at 234 nm for the production of conjugated diene monohydroxylated products. The 17S-HpDHA and 17S-HDHA reactions were monitored at 270 nm for the production of conjugated triene dihydroxylated products.

[b]Relative k_{cat}/K_M values with DHA were set to 1.

Table 7.

Effective k_{cat}/K_M (k_{cat}/K_M × percent product at 270 nm) Values of 16S,17S-EpoxyDHA for Reaction of h-12-LOX and h-15-LOX-1 with 2 μM 17S-HpDHA

	16S,17S-epoxyDHA effective k_{cat}/K_M	**relative 16S,17S-epoxyDHA effective k_{cat}/K_M [a]**
h12-LOX	0.0075	1
h15-LOX-1	0.41	55

[a]The relative 16S,17S-epoxyDHA effective k_{cat}/K_M for the h-12-LOX + 17S-HpDHA reaction was set to 1.

Table 8.

Effective k_{cat}/K_M (k_{cat}/K_M × percent product at 270 nm) of PDX for Reaction of h12-LOX and h15-LOX-1 with 17S-HpDHA and 17S-HDHA

enzyme	substrate	PDX effective k_{cat}/K_M	relative PDX effective k_{cat}/K_M [a]
h12-LOX	17S-HpDHA	0.0078	1
h12-LOX	17S-HDHA	0.0013	0.17
h15-LOX-1	17S-HpDHA	0.21	27
h15-LOX-1	17S-HDHA	0	0

[a]The relative PDX effective k_{cat}/K_M for the h-12-LOX + 17S-HpDHA reaction was set to 1.